LAST MILLENNIUM REGIONAL CLIMATE ANOMALIES: CENTRAL AMERICA AND THE MIDDLE EAST

Yochanan Kushnir

LDEO/CMG GloDecH Meeting

Wednesday, February 8, 2012

OUTLINE

- LIA to modern climate transition in Central America: evidence of volcanic and solar forcing
    - *Background*
    - *Proxy records of hydroclimate change*
    - *Comparison with estimates of volcanic and solar forcing*
- Documentary evidence of Levant droughts during the medieval era (work with Kate Rephael and Mordechai Stein from the Hebrew University of Jerusalem)
    - *Background*
    - *Documentary evidence of droughts*
    - *Comparison to the Nile flood record*

LIA TO MODERN CLIMATE TRANSITION IN CENTRAL AMERICA: EVIDENCE OF VOLCANIC AND SOLAR FORCING

Work with Amos Winter, Thomas Miller, and Juan Estalla from the University of Puerto Rico at Mayaguaze and David Black from Stony Brook University

This study presents and analyzes the findings from an annually resolved time series of $\delta^{18}O$ derived from a speleothem extracted from a cave close to the Guatemala-Belize boarder at 17°N, 89°13'W (red star below). The region is projected to dry in the future under the influence of GHG increase and resolving its long-term climatic variations in the past is important for putting the future drying in context.

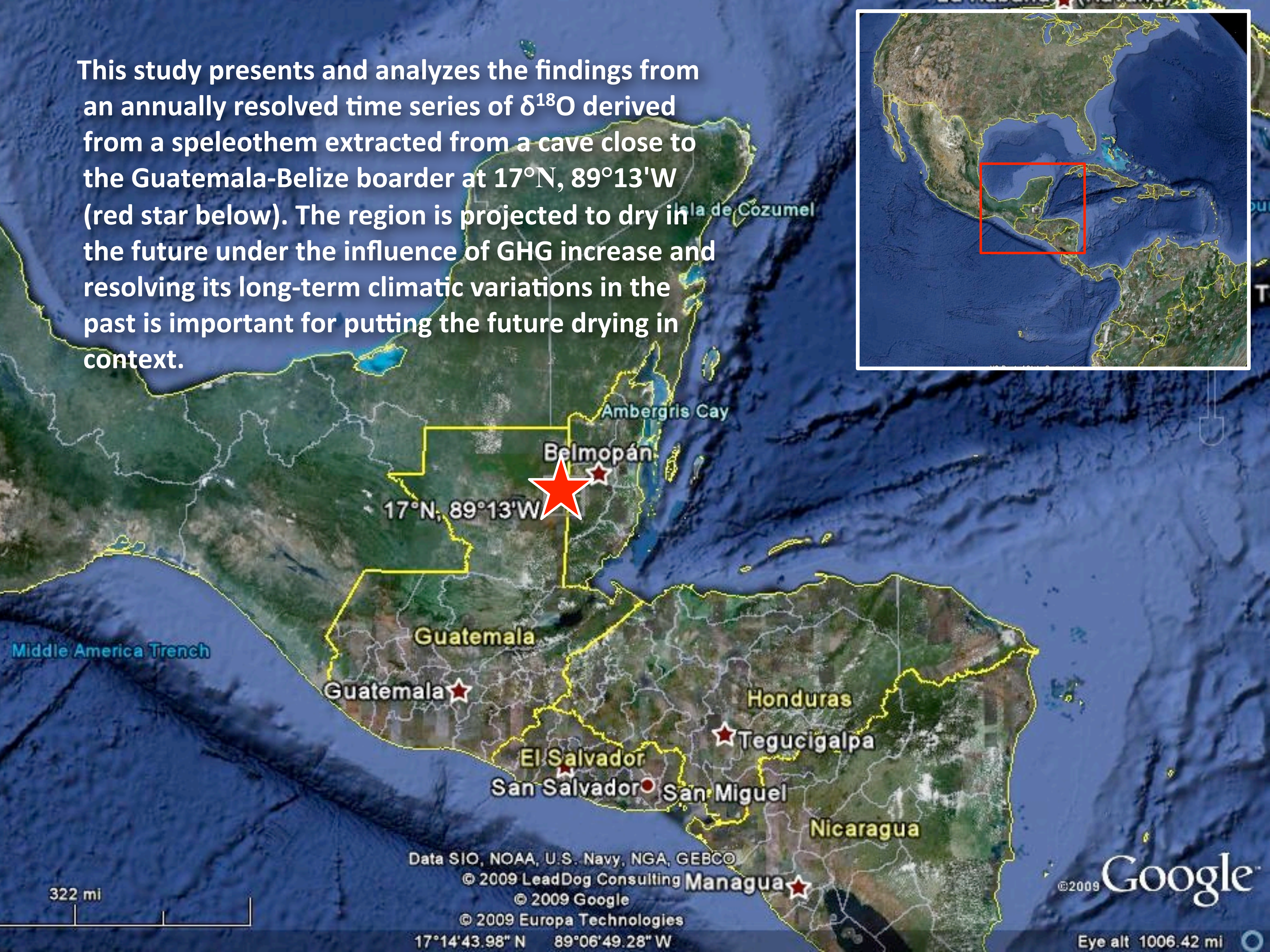

The Guatemala Speleothem

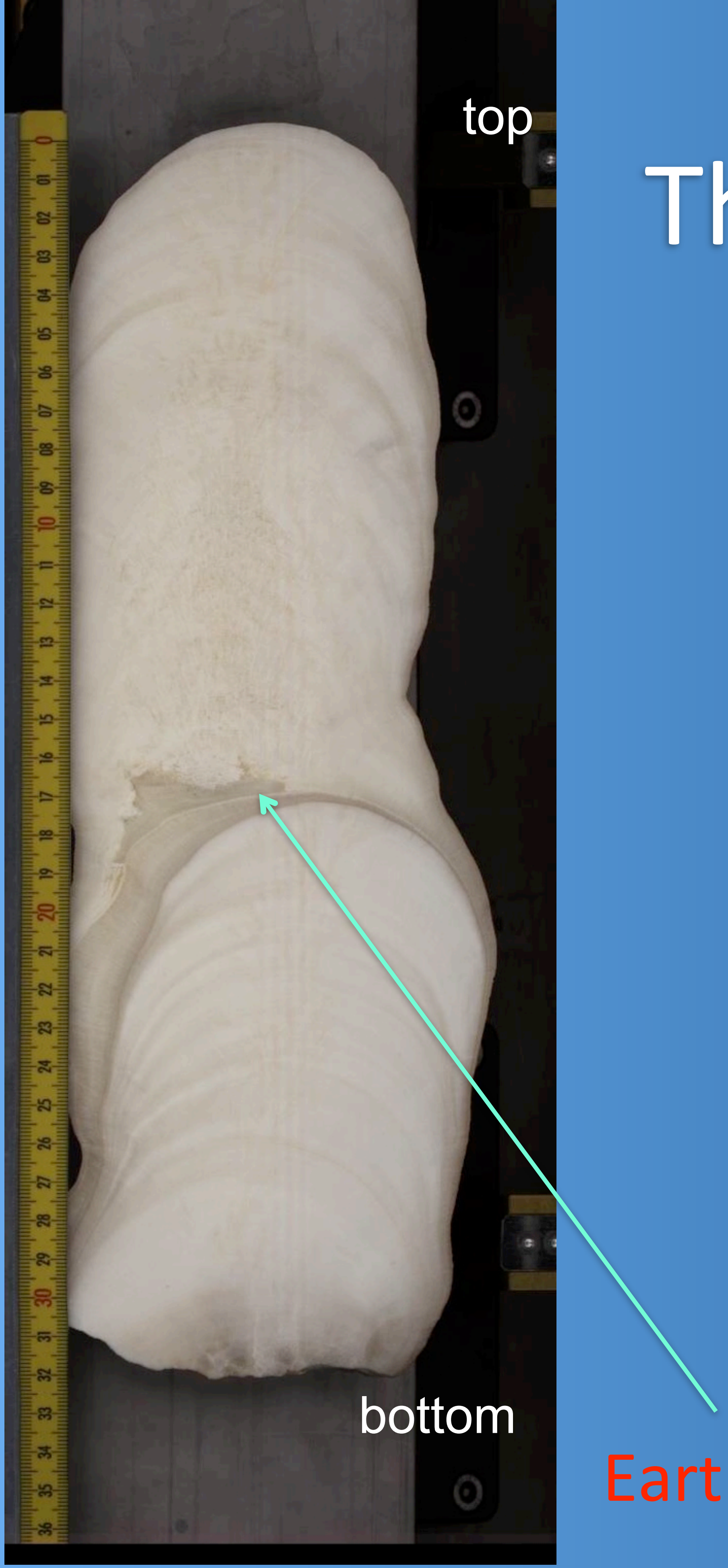

Earthquake 1541

- The speleothem present two growth segments separated by a long break.
- The figure on the left displays change in growth axis during the growth hiatus
- A particularly devastating earthquake struck the region in 1541, in the middle of the growth hiatus. The quack was large enough to destroy the capital of Guatemala, ~300 km away

The Guatemala Speleothem

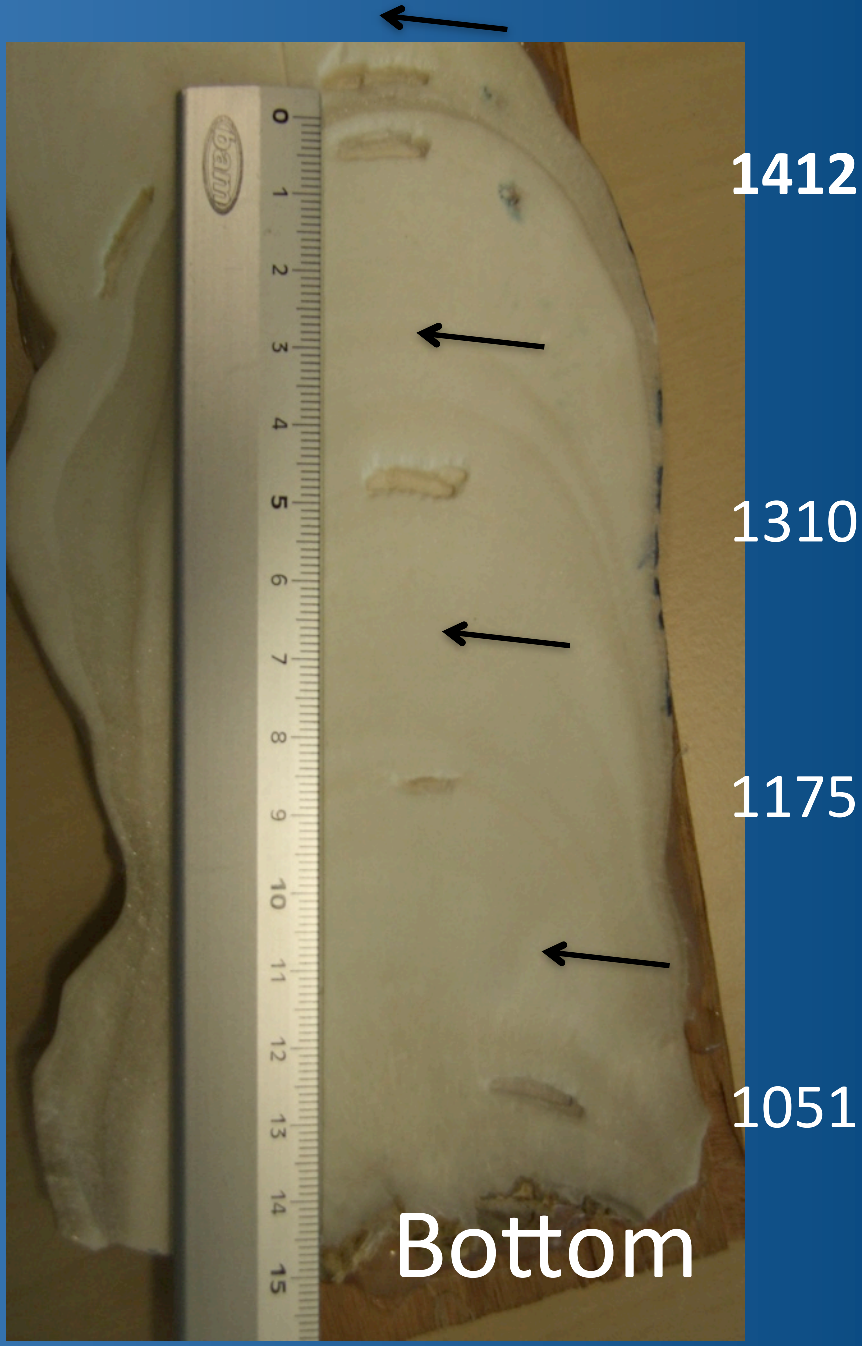

Mayan Post Classical Period

Growth rate = .625mm per year

The δ18O record

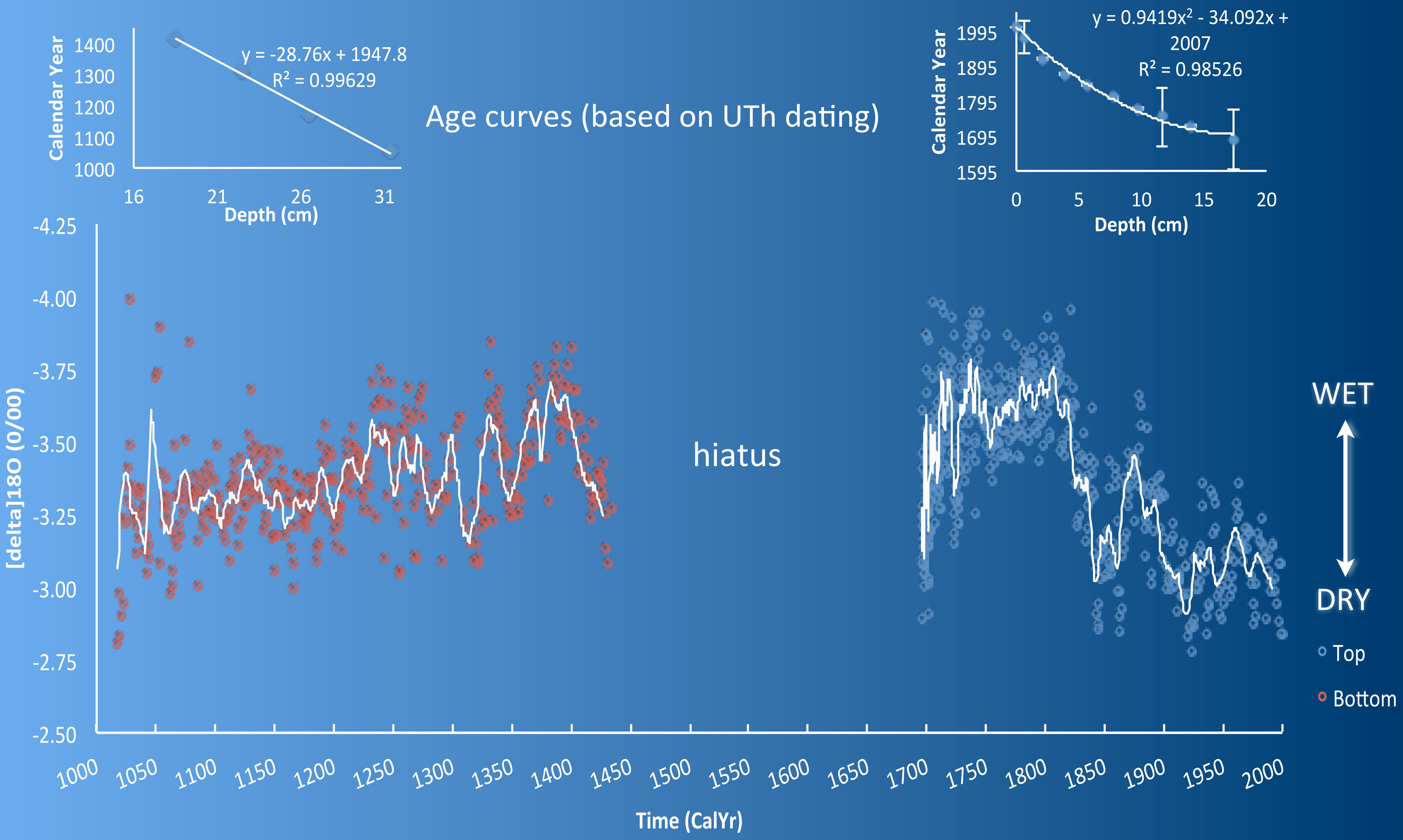

Correlation Speleothem $\delta^{18}O$ & rainfall

The speleothem $\delta^{18}O$ correlates with local rainfall during the summer season. The lag may be partly a delayed integrating response but may partly be due to dating uncertainties).

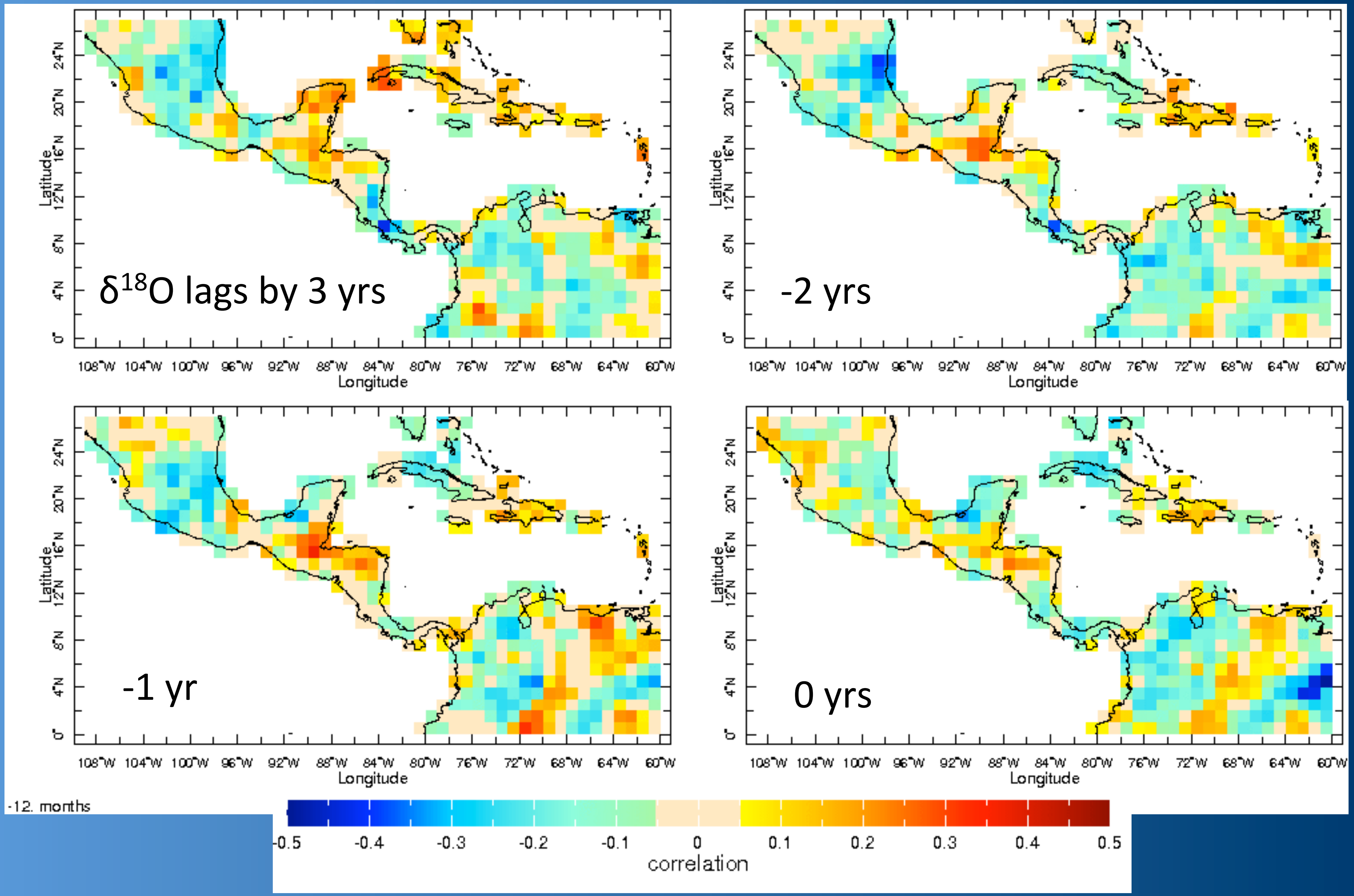

EOF of MesoAmerica rainfall

Rotated EOF analysis of Jun-Oct precipitation anomalies in MesoAmerica (data - CRU TS 3.1 analysis of rain gauge observations 1920-2009).Speleothem cave location is marked by bold rectangle.

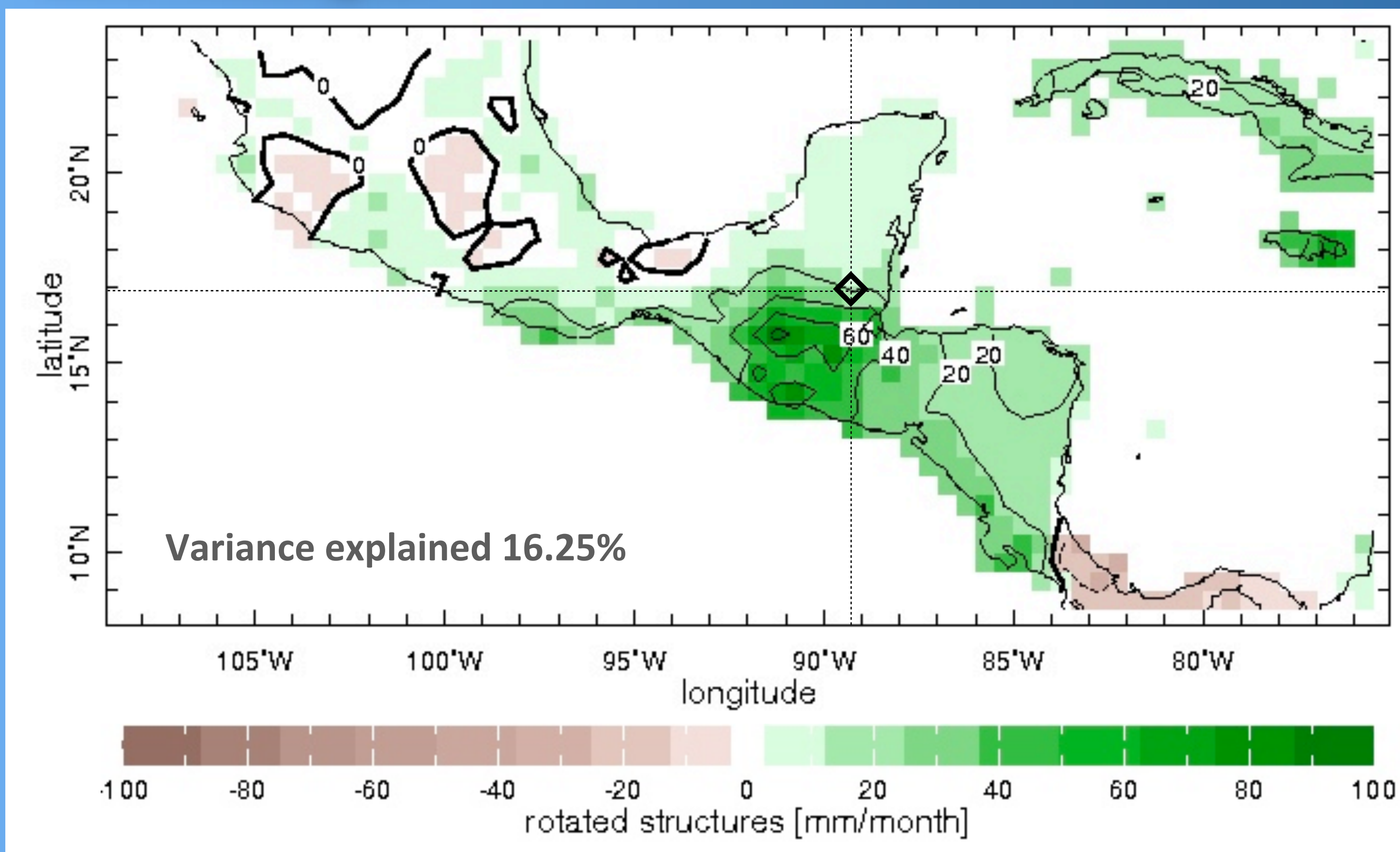

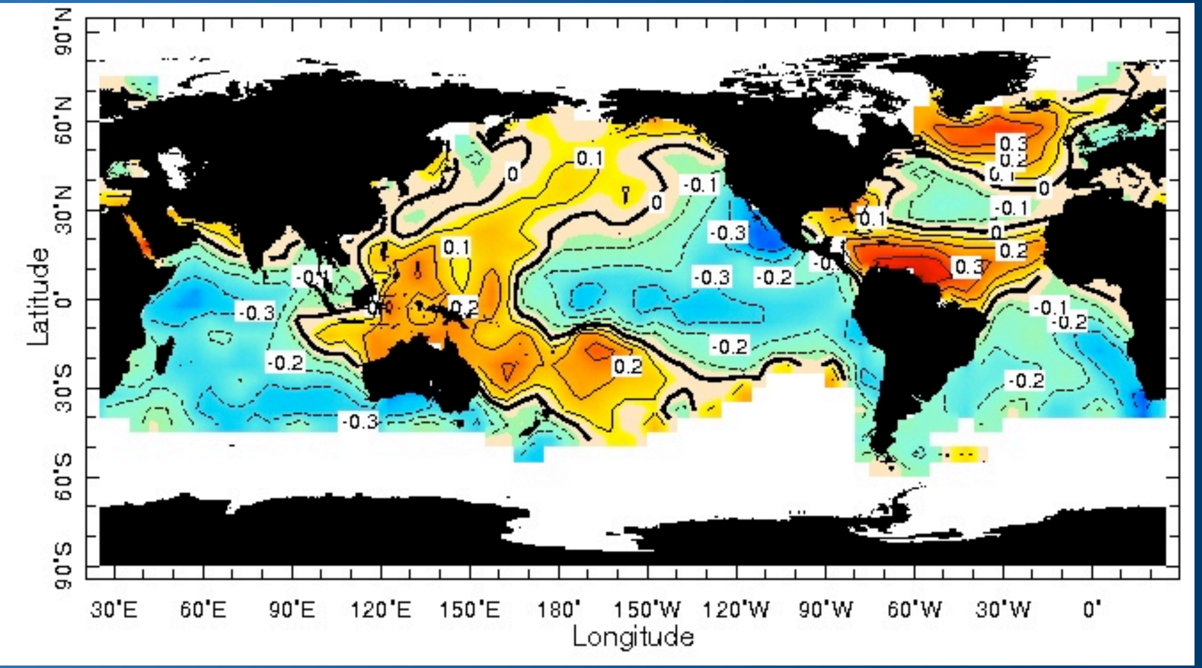

Correlation between the EOF time series and global SST anomalies. The Guatemalan highlands receive more rain than normal when the Atlantic SSTA is pos and the E. Pacific SSTA is neg.

EOF time series (in red) & the negative of the speleothem δ^{18}O. The correlation (r=0.26) is largest when the rainfall series is leading the speleothem by 1 year. The speleothem integrates the seasonal rainfall variations.

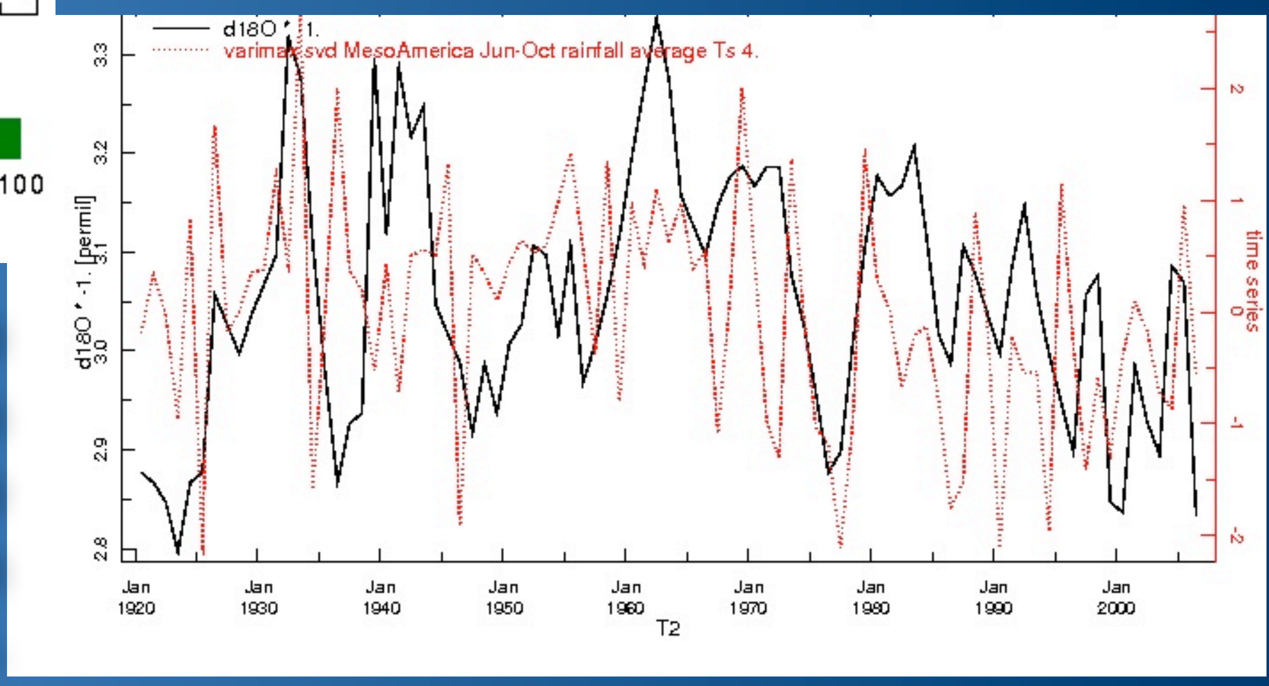

Correlation Speleothem $\delta^{18}O$ & SST

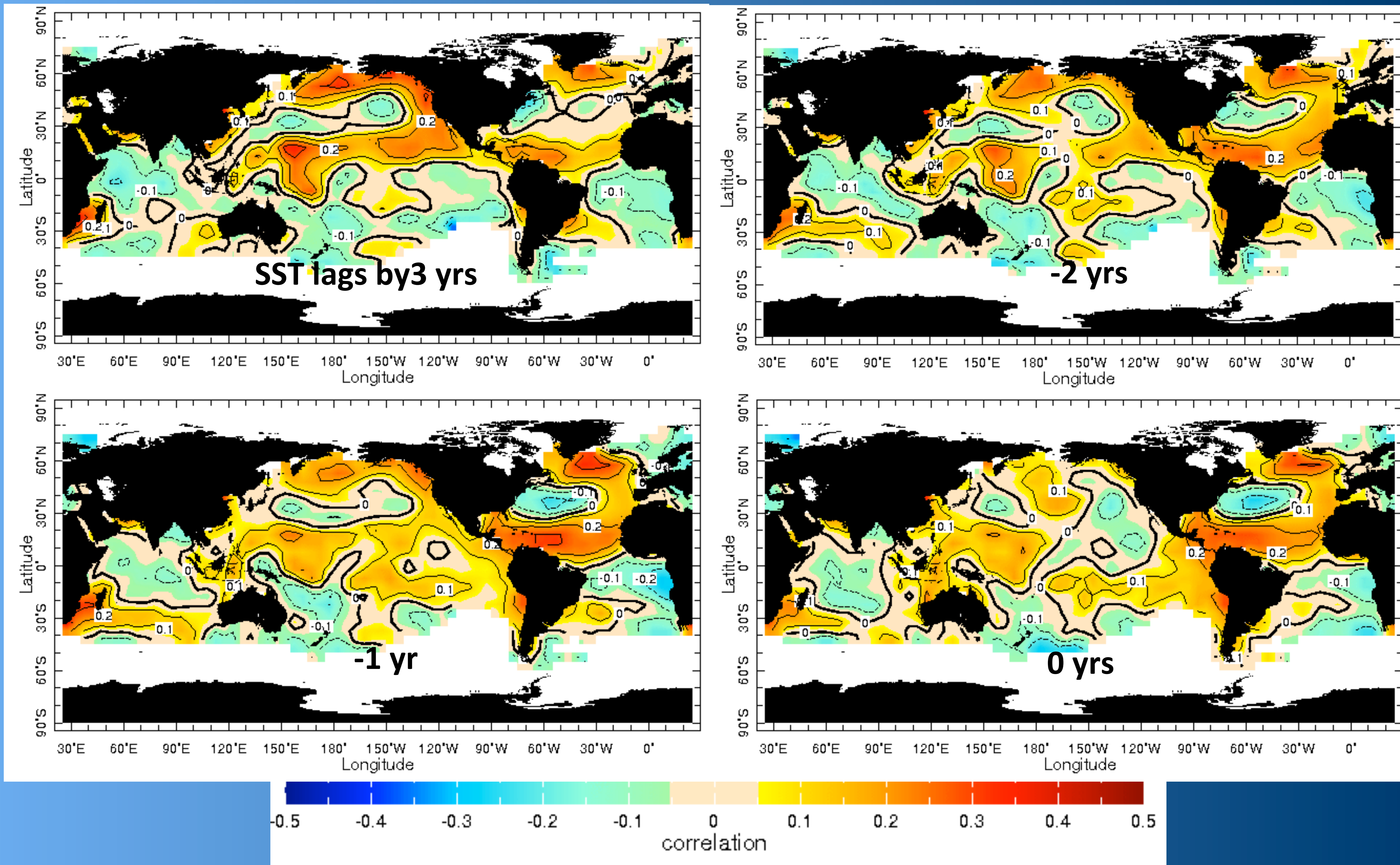

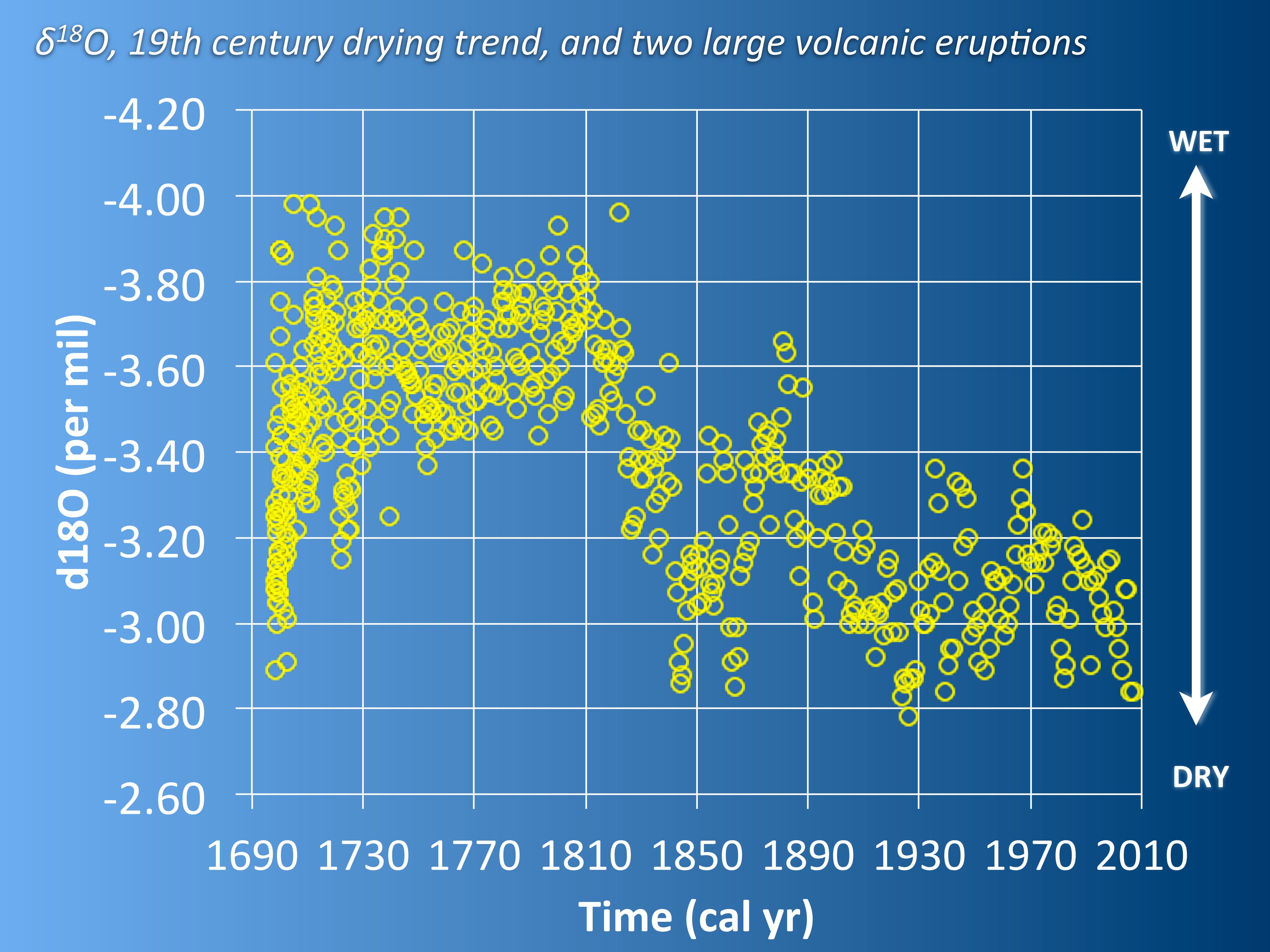
δ18O, 19th century drying trend, and two large volcanic eruptions
d18O (per mil)
-4.20
-4.00
-3.80
-3.60
-3.40
-3.20
-3.00
-2.80
-2.60
1690
1730
1770
1810
1850
1890
1930
1970
2010
Time (cal yr)
WET
DRY

$\delta^{18}O$, 19th century drying trend, and two large volcanic eruptions

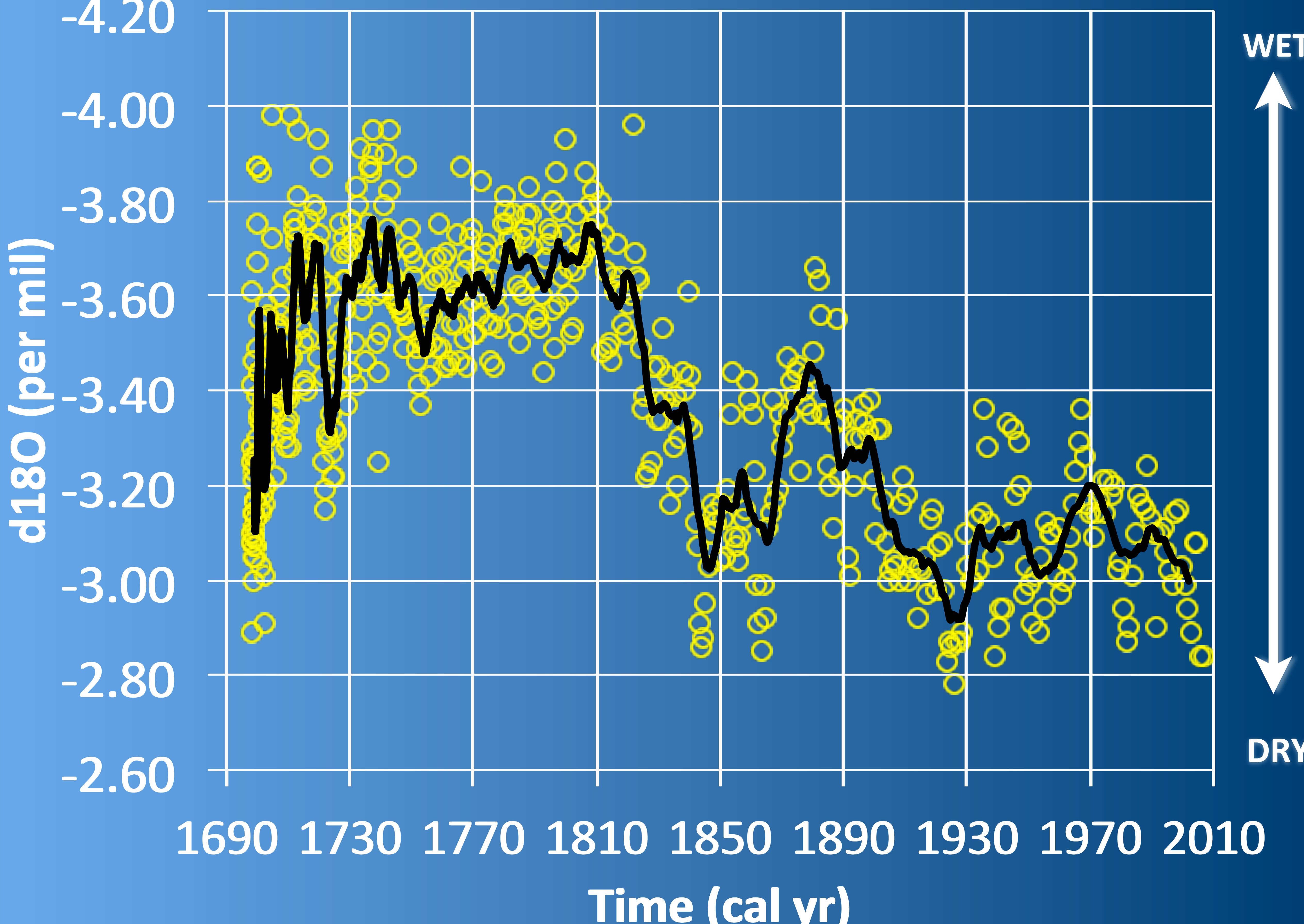

$\delta^{18}O$, 19th century drying trend, and two large volcanic eruptions

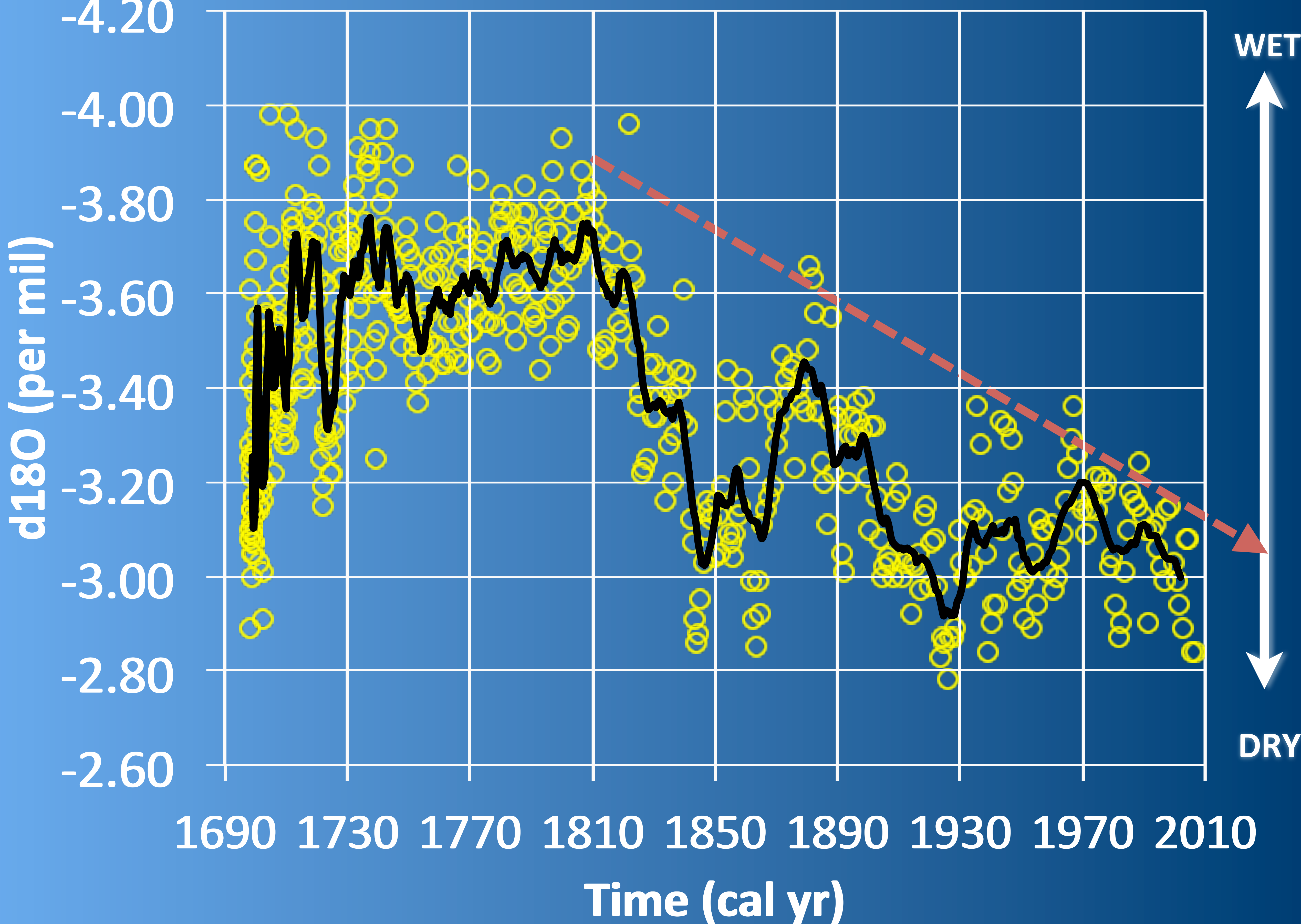

$\delta^{18}O$, 19th century drying trend, and two large volcanic eruptions

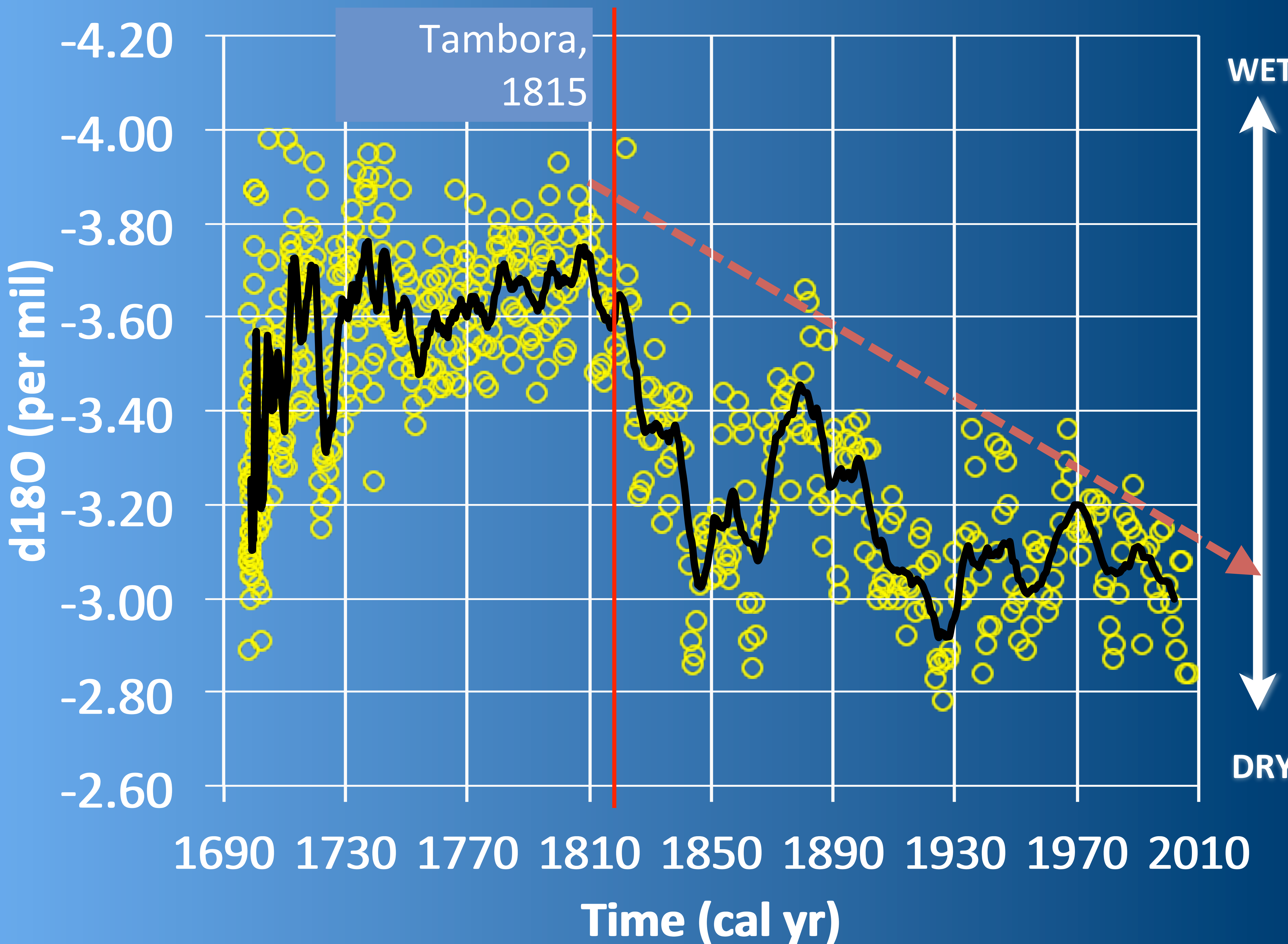

$\delta^{18}O$, 19th century drying trend, and two large volcanic eruptions

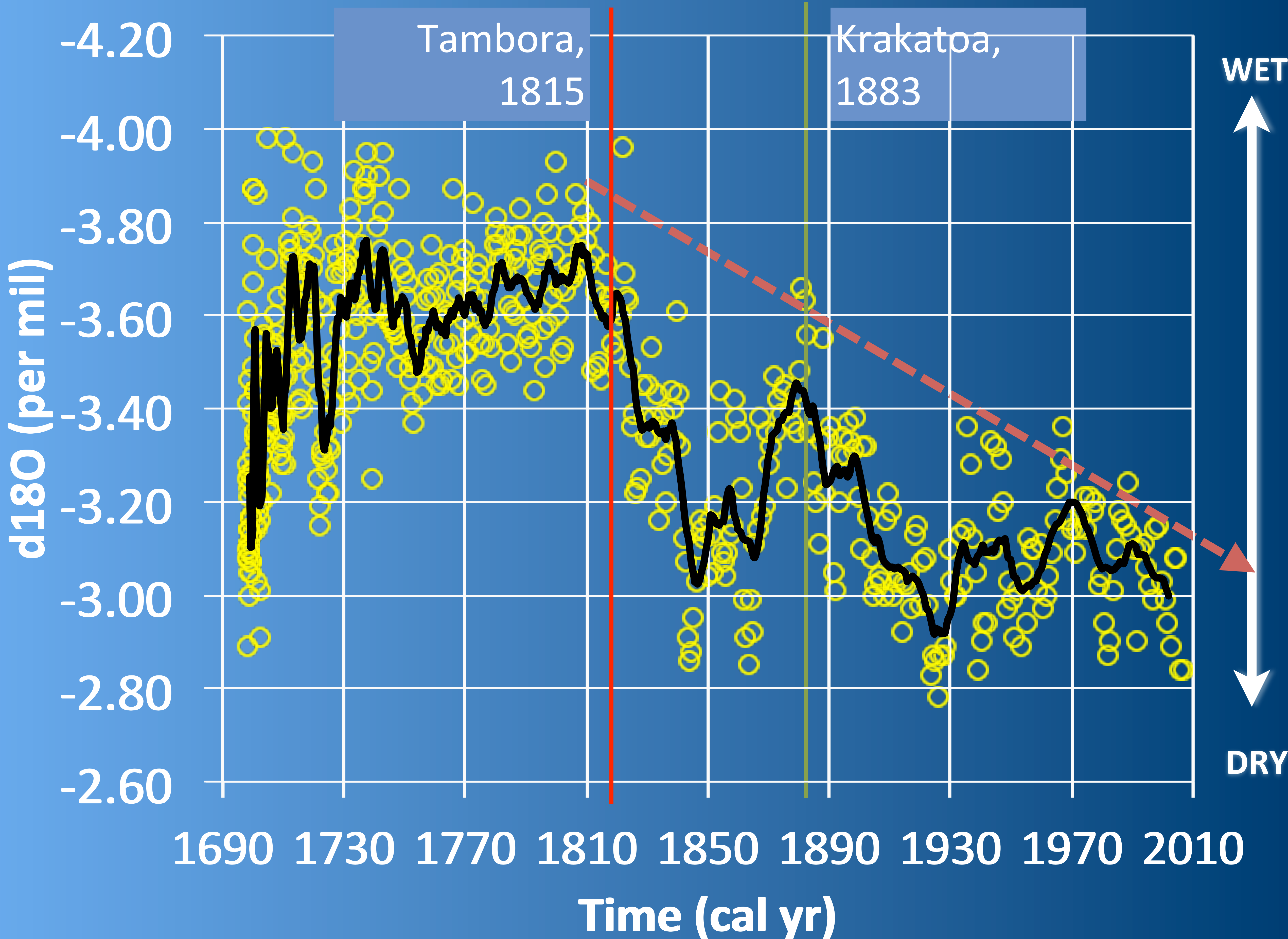

Tambora eruption: the world's largest historical eruption with explosive index 7, occurred in April 1815.

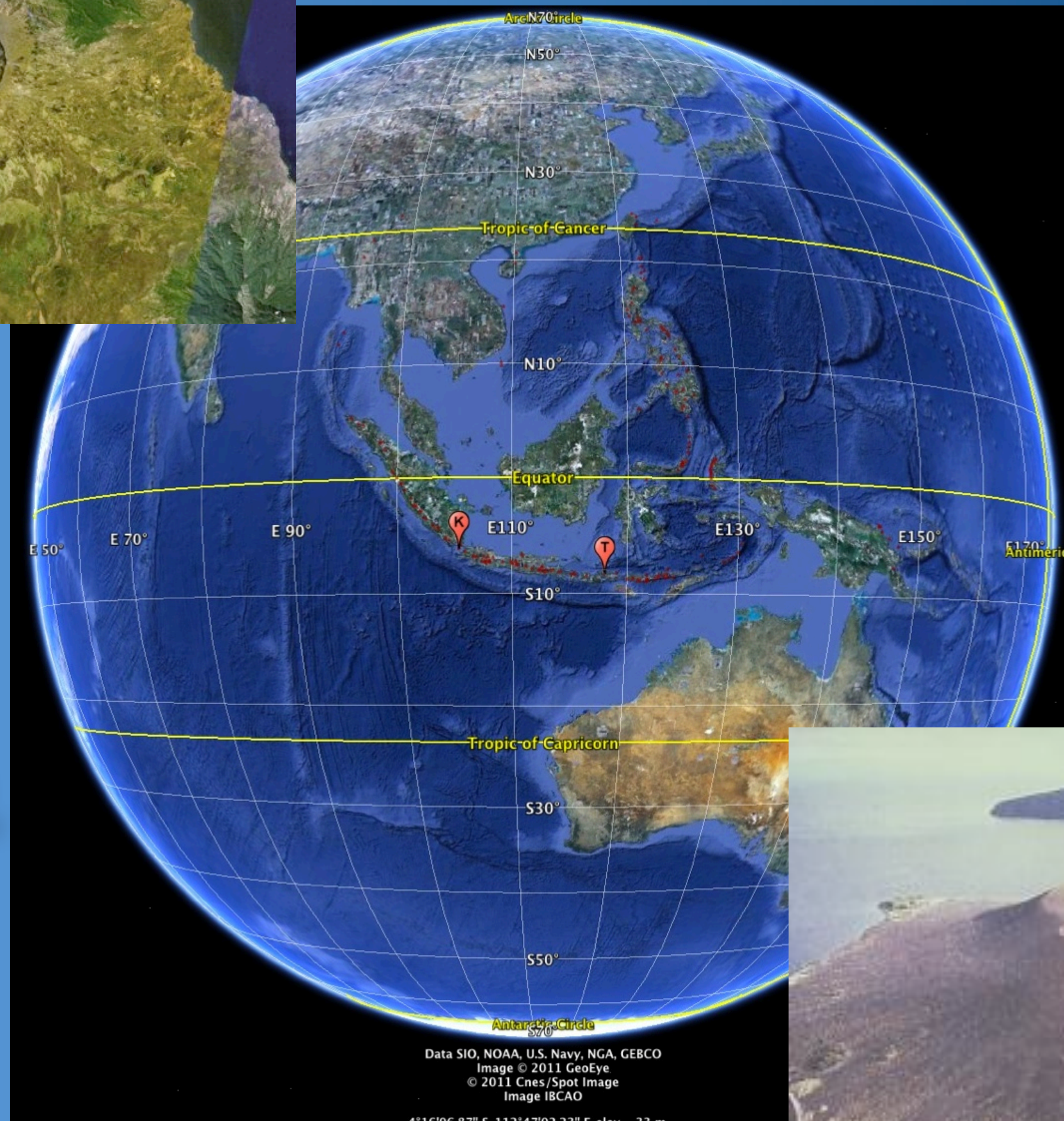

Krakatoa eruption: Explosive index 6, occurred in August 1883

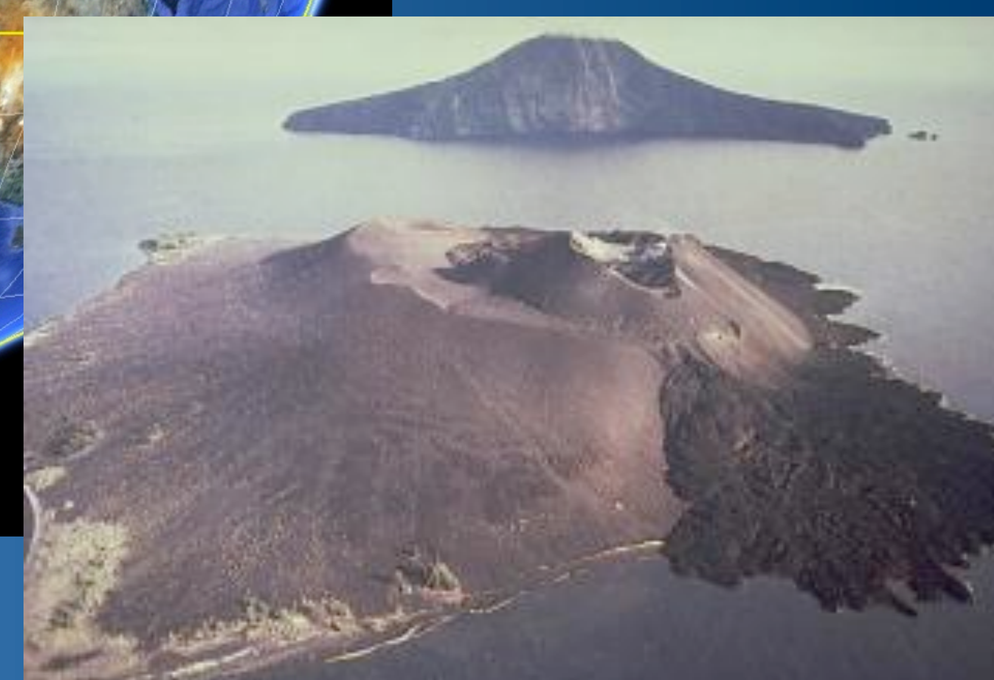

Krakatau

Historical Volcanic Eruptions

Volcano	Year	VEI	d.v.i/E_{max}	IVI
Lakagígar [Laki craters], Iceland	1783	4	2300	0.19
Unknown (El Chichón?)	1809			0.20
Tambora, Sumbawa, Indonesia	1815	7	3000	0.50
Cosiguina, Nicaragua	1835	5	4000	0.11
Askja, Iceland	1875	5	1000	0.01*
Krakatau, Indonesia	1883	6	1000	0.12
Okataina [Tarawera], North Island, NZ	1886	5	800	0.04
Santa María, Guatemala	1902	6	600	0.05
Ksudach, Kamchatka, Russia	1907	5	500	0.02
Novarupta [Katmai], Alaska, US	1912	6	500	0.15
Agung, Bali, Indonesia	1963	4	800	0.06
Mt. St. Helens, Washington, US	1980	5	500	0.00
El Chichón, Chiapas, Mexico	1982	5	800	0.06
Mt. Pinatubo, Luzon, Philippines	1991	6	1000	—

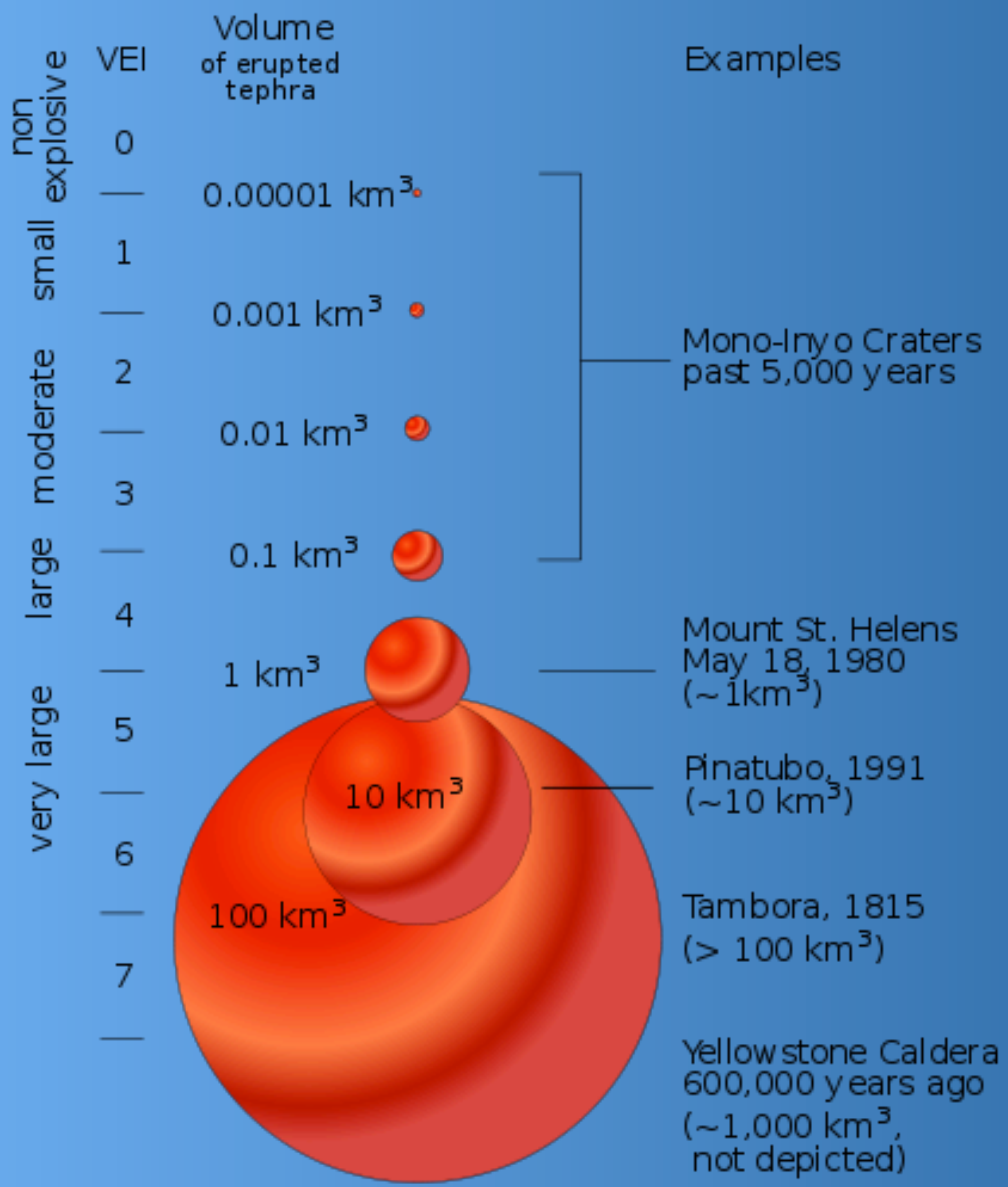

The eruption of Mt. Krakatoa (1888 English lithograph)

VEI scale

source: http://volcanoes.usgs.gov/Products/Pglossary/vei.html

Forcing and signal

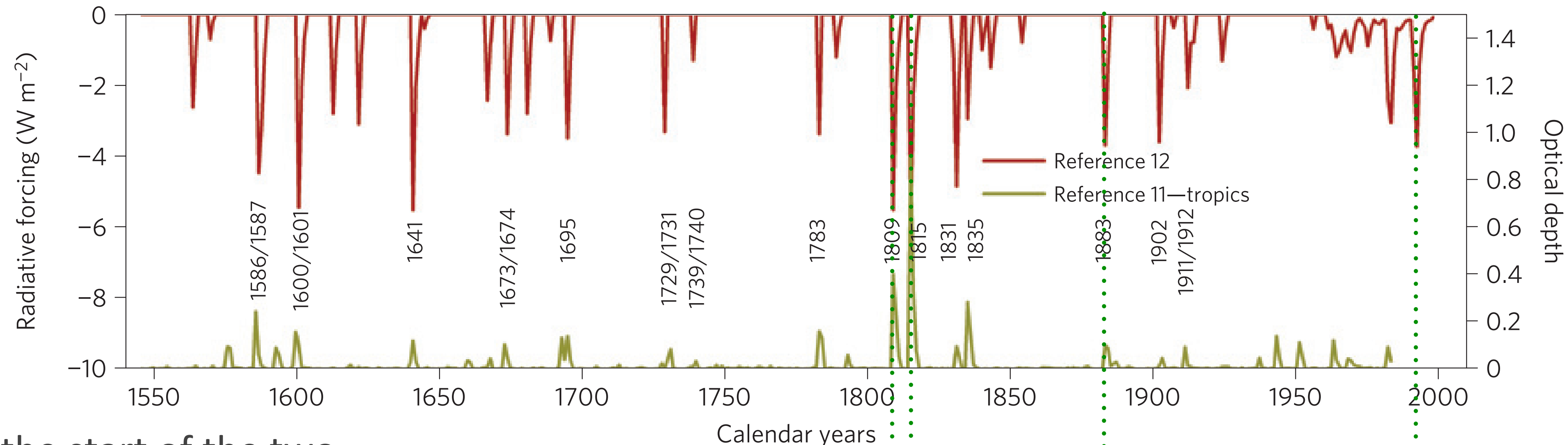

The close relation between the start of the two 19th century drying trends and the timing of large volcanic eruption is more than a mere coincidence, for the following reasons:

- *The volcanic dust veil generated by the early- and late-19th century eruptions was considerable (next slide).*
- *Recent GCM experiments (second following slide) suggest that we can expect such large eruptions to generate a forced climatic response that includes a protracted, tropic-wide cooling of sea surface temperatures. This would result in the persistent drying of Meso-America.*

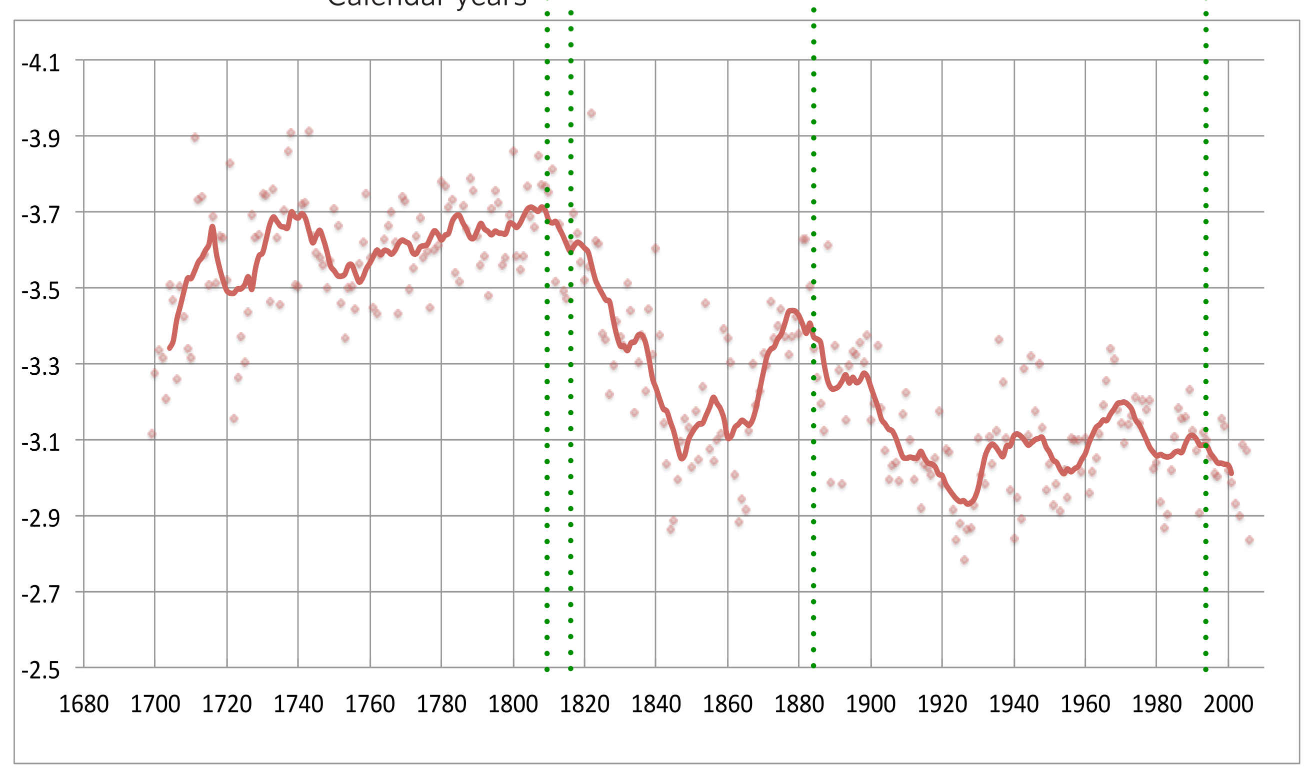

Persistence due to volcanic forcing

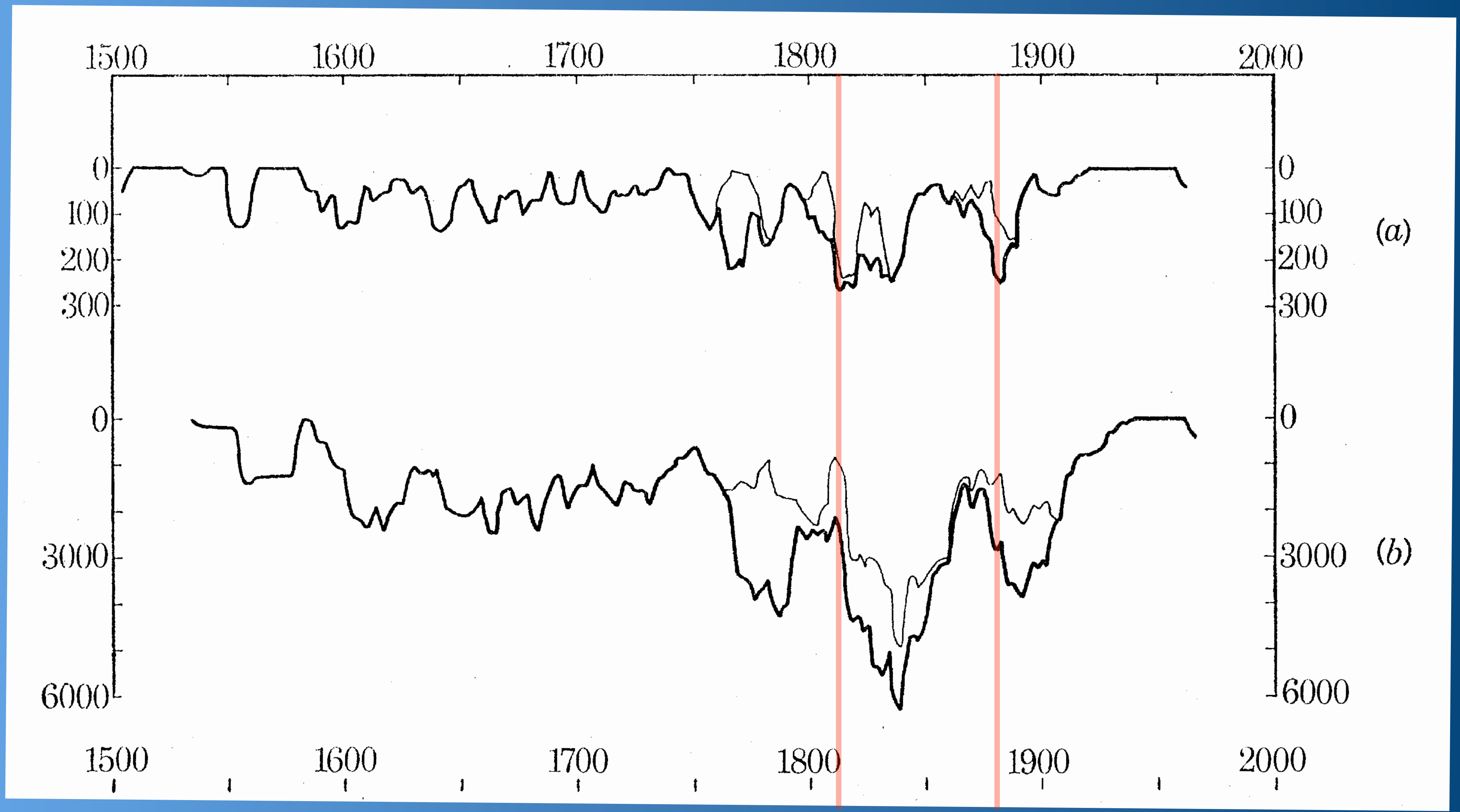

Volcanic dust over the northern hemisphere (a) 10-year running mean values of d.v.i. plotted against the middle of the decade. (b) 25-year cumulative d.v.i. In (a) and (b) the finer line indicates values obtained by ignoring cases of dust veils assessed solely on evidence of temperature anomaly. (Source: Lamb, 1970)

Response to large volcanic eruptions

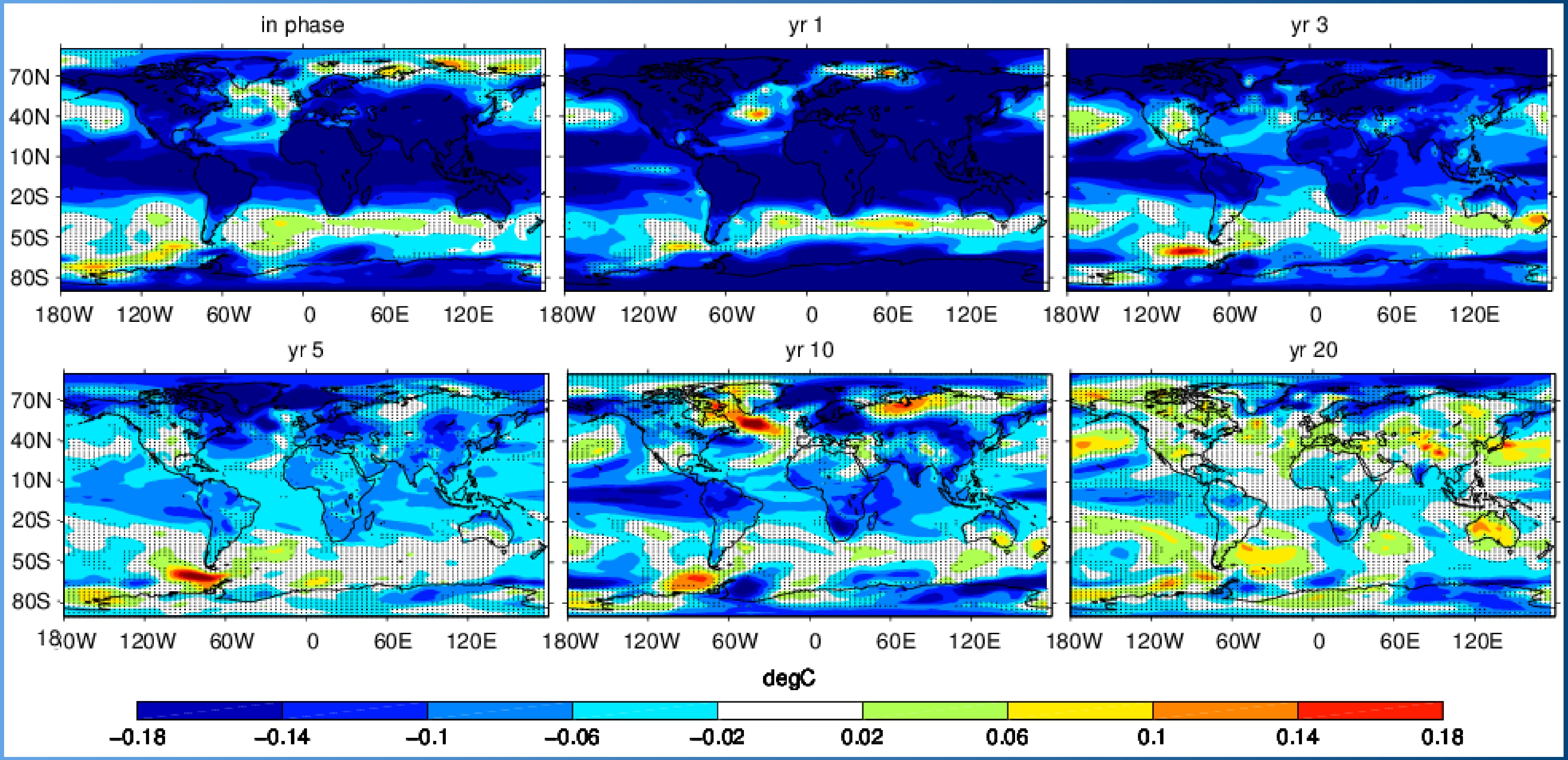

Composites of annual mean surface temperature with respect to volcanic eruptions with corresponding to optical depths higher than 0.15. Surface temperature corresponds to SST over the ocean and air temperature otherwise. Dotted areas are *not significant* at the 5 % level. The composites are in-phase and at lags between 1 and 20 years

Source: Mignot et al. (2011)

The solar record

Another prominent source of external forcing are the changes in Total Solar Irradiance (TSI) that were quite large during the LIA and into the early industrial age. Here are several estimates based on different proxies and/or methods used to reconstruct these TSI variations. The two minima that affected the 19th century are the Dalton minimum, which reached its extreme state between 1810 and 1830 (depending on the reconstruction method) and an unnamed, much weaker minimum peaking around 1900. The mechanisms and relative role of TSI fluctuations in climate are debated in the old and new literature. However, this forcing may have also played a role in Meso-America hydroclimate variability that is captured by the Yucatan speleothem.

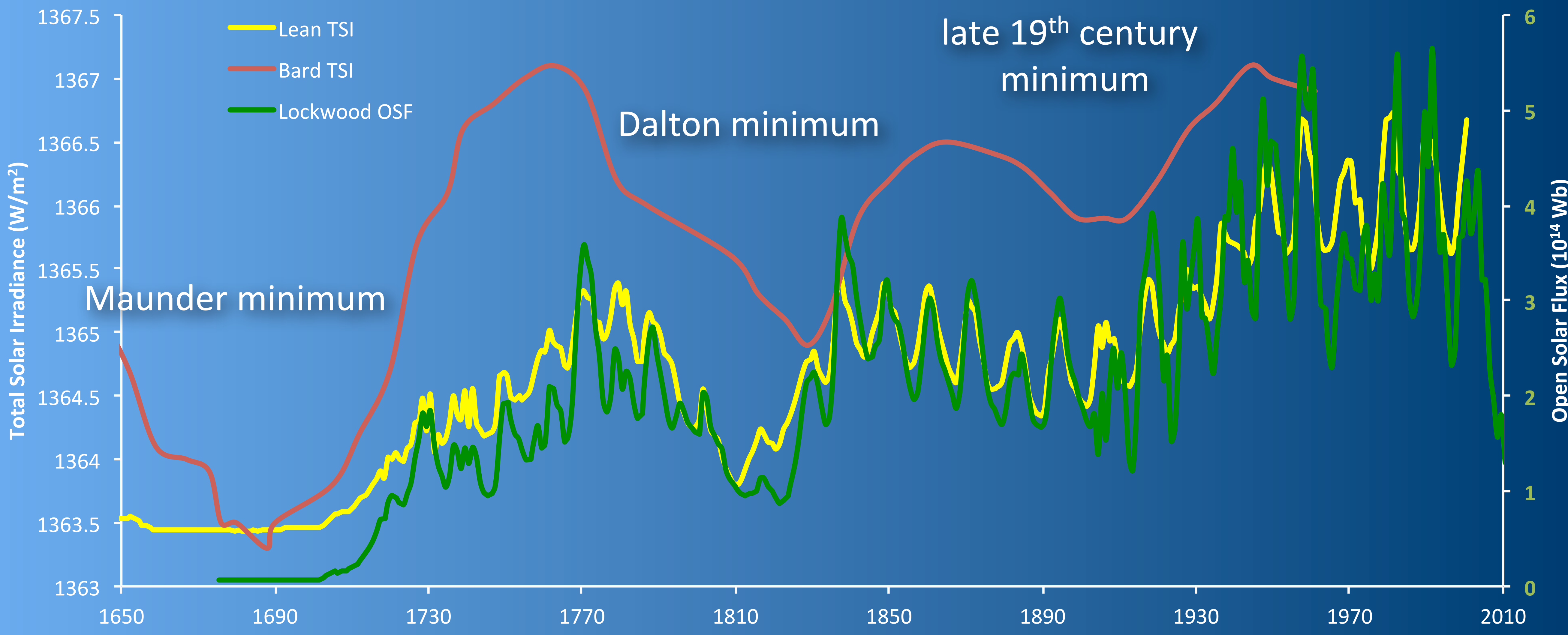

Climate forcing of last millennium monsoons

Smoothed time series of the (a) solar radiative forcing (W m2), (b) volcanic effect (W m2), (c) effective solar radiation (W m2), (d) CO2 concentration (ppm), and (e) Global Monsoon Index (mm day). All time series are 31-yr running means from AD 1000 to 1990. The numbers shown in the lower-right corners indicate correlation coefficients of GMI with the four external forcing factors and two temperature indexes, respectively. Source: Liu et al. (2009)

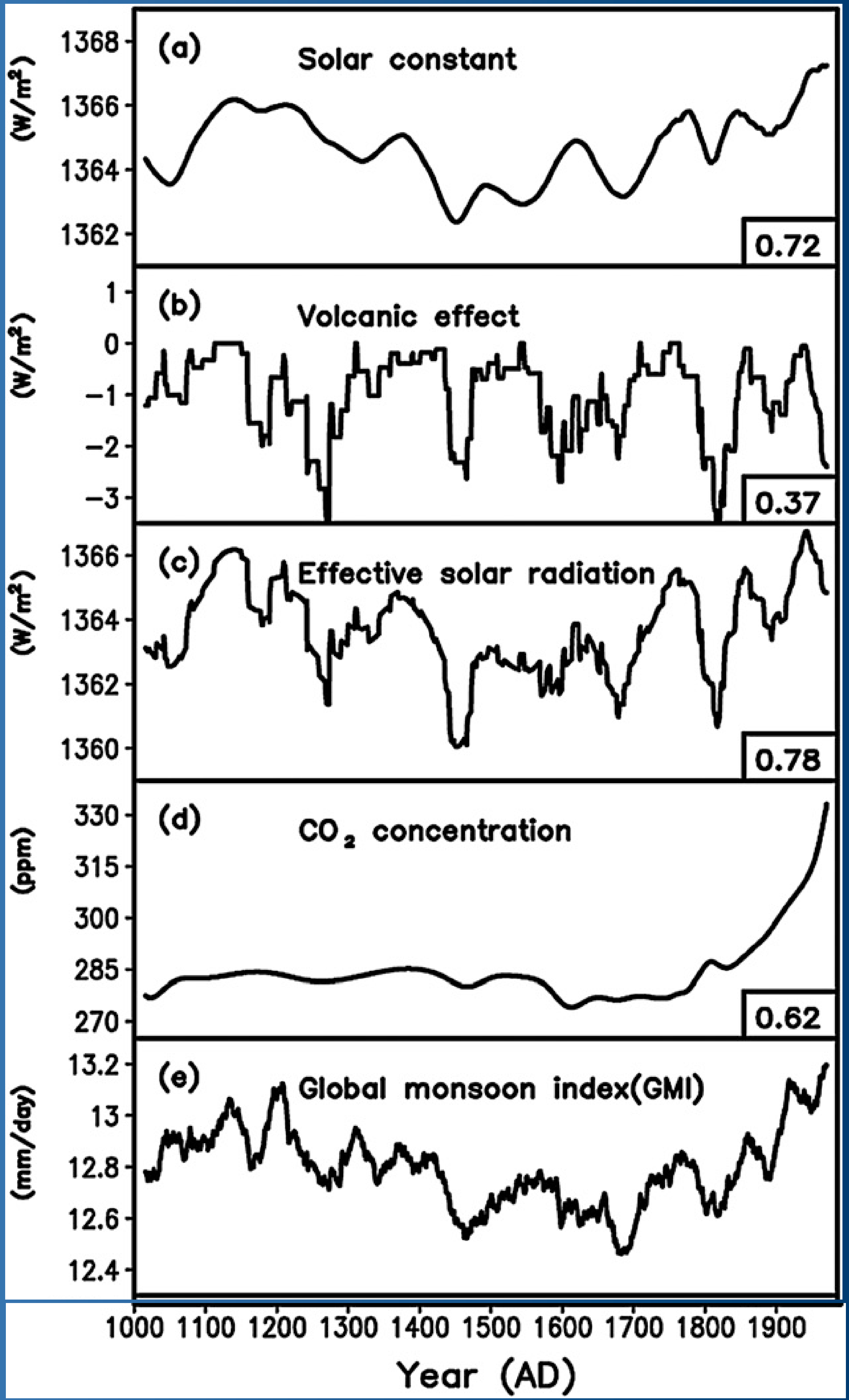

LIA cooling

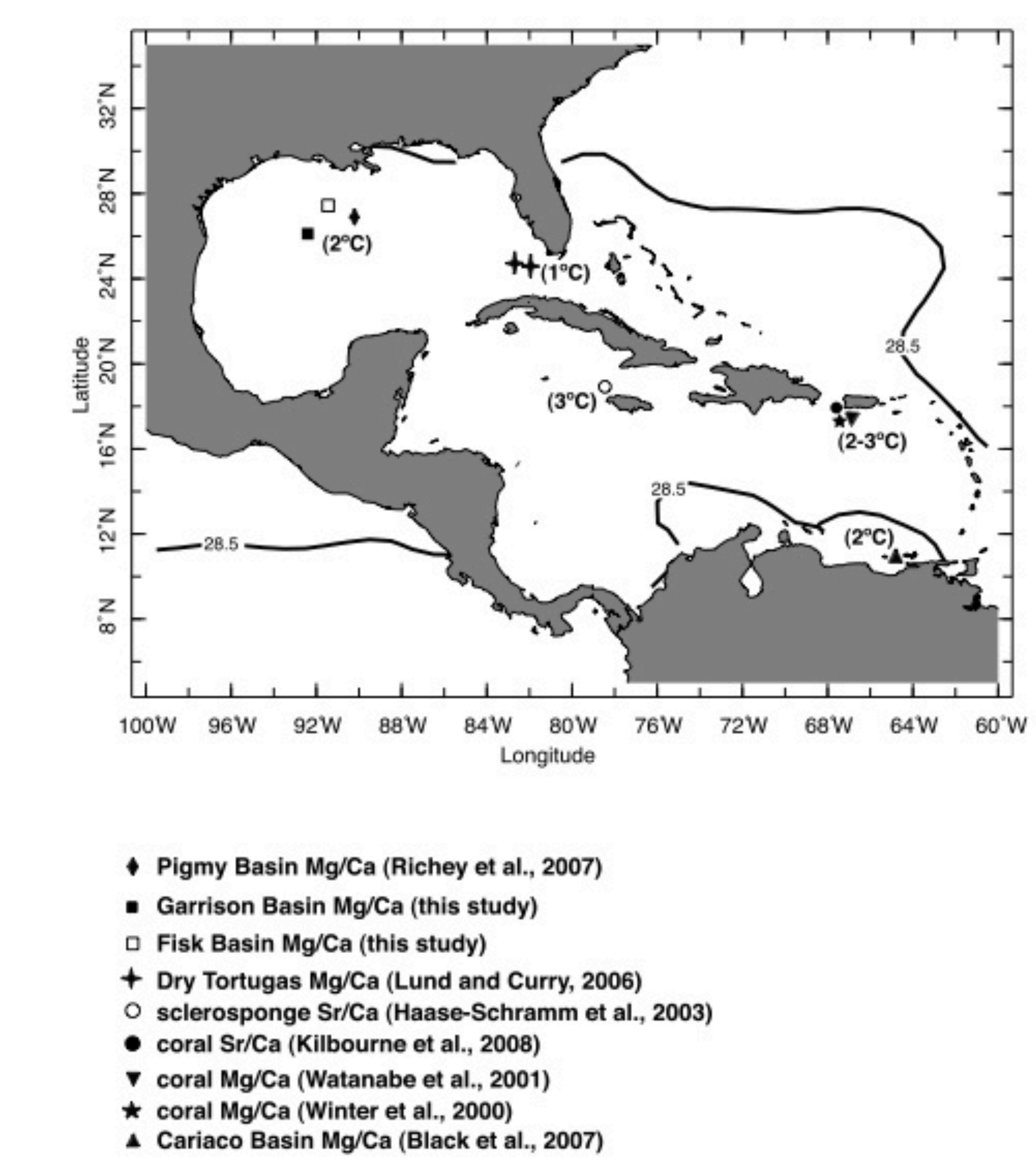

Map of proxy records in the GOM-Caribbean region exhibiting 1–3°C cooling during the LIA. The September (maximum seasonal geographic extent) AWP (28.5°C isotherm) is plotted using the Reynolds and Smith OISST V2.0 dataset averaged from 1981 to 2009. Mean LIA *cooling* is indicated in parentheses for each region. Source: Richey et al. (2009)

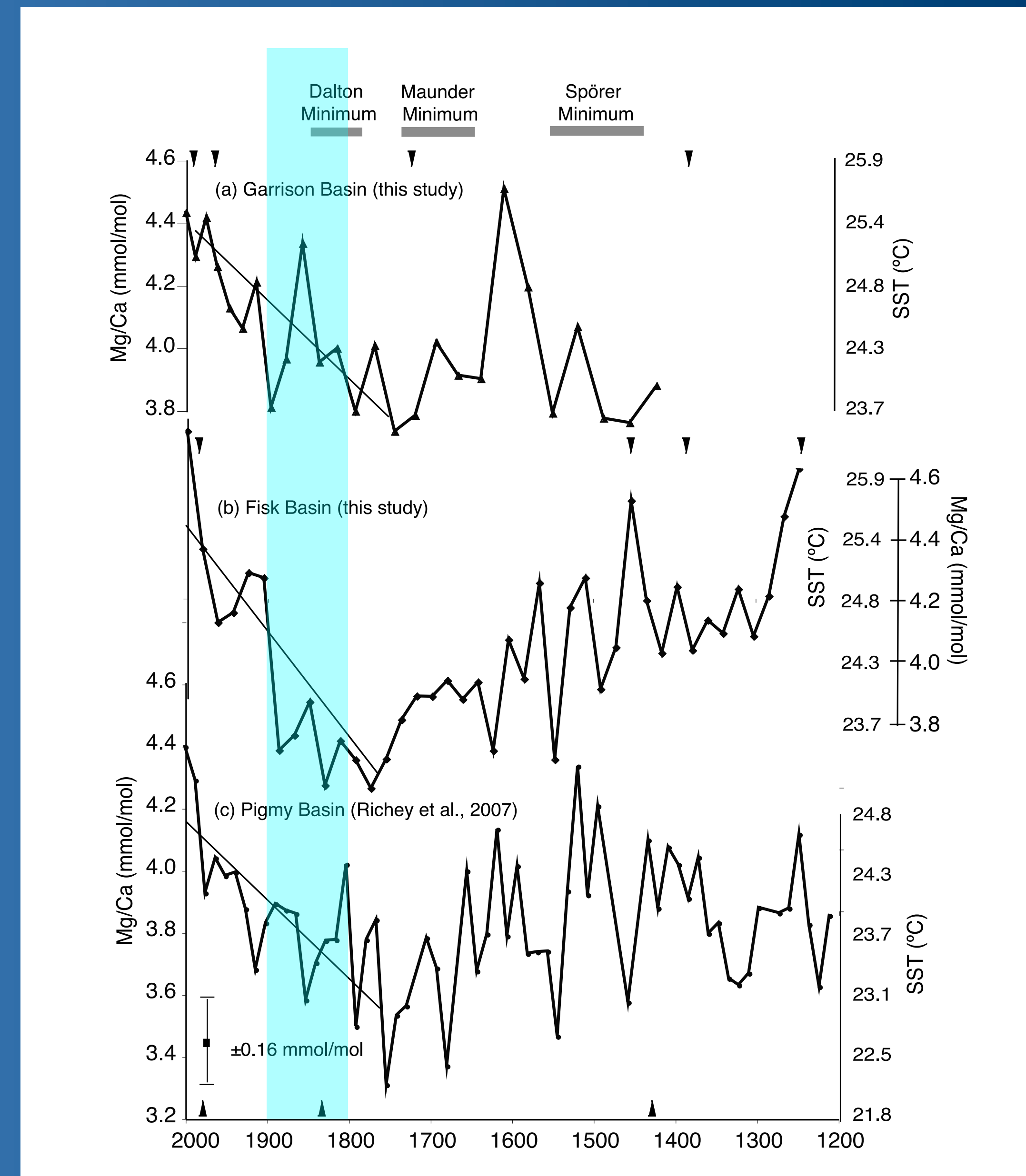

Maximum cooling was observed during the 18th century (during the Maunder Minimum), and the region was warming in the 18th century. The 19th century is highlighted. The peak cooling relationship to our speleothem record is not obvious and may be difficult to resolve due to dating and resolution issues.

Conclusions

- We have a well-dated, high resolution speleothem $\delta^{18}O$ record, which is located in a key location in Central America. Unfortunately the record is broken into two parts by a three-century hiatus that spans a large part of the LIA.
- The 19th century record displays two persistent ~30 year drying trends which occurred immediately after the two largest volcanic eruptions of the century.
- The eruptions occurred at the same time that the region may have been reacting to recorded minima in solar irradiance. These could have added to the persistent drying. However, the long delay of the hydroclimatic response w.r.t. the solar minima remains to be explained
- The speleothem drying occurs when the Caribbean and Gulf of Mexico are warming from a deep minimum in the 18th century.
- The region may be exceptionally climate-sensitive because it is straddled the Atlantic and Pacific Oceans, which through their SST state determine the location of the summer ITCZ.
- The exact climate mechanisms need to be determined by last-millennium model integrations.

DOCUMENTARY EVIDENCE OF LEVANT DROUGHTS DURING THE MEDIEVAL ERA

Work with Kate Rephael and Mordechai Stein, the Hebrew University of Jerusalem

BACKGROUND: THE MODERN CLIMATE

Jerusalem rainfall and the Atlantic Multidecadal Oscillation

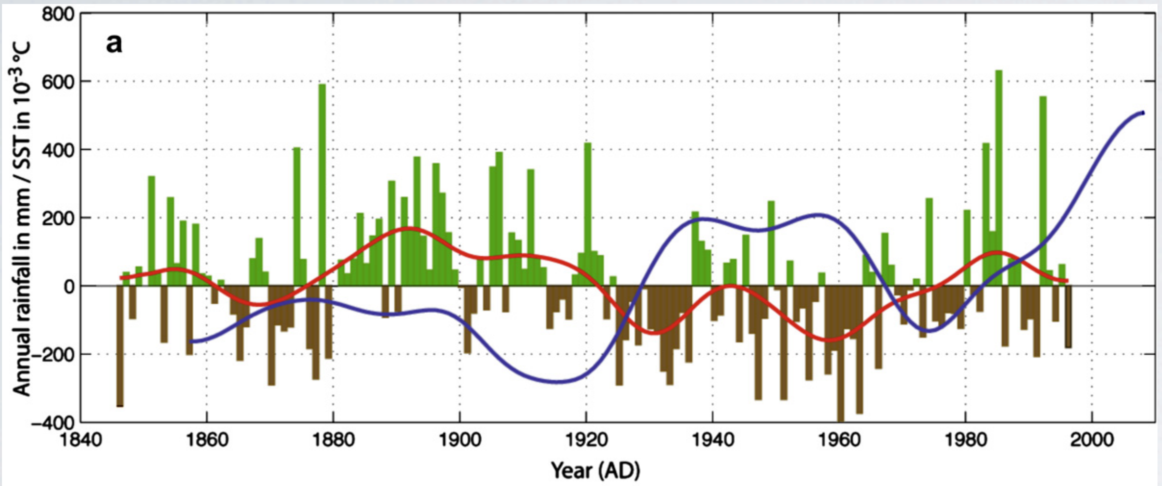

Annual (October-September) measured anomalous precipitation in Jerusalem with respect to the 1961-1990 climatology (color bars in mm) and its low-pass filtered counterpart (in red). Also shown (in blue) are the low-pass filtered SSTA averaged over the extratropical North Atlantic (30N to 70N) in units of 10^{-3} °C. The low-pass filtered curves emphasize fluctuations with a period of 20 years and longer. Station precipitation is from the NOAA Global Historical Climatology Network (GHCN) dataset and SST is from the Kaplan analysis.

Jerusalem - Sahel anti-phase correlation

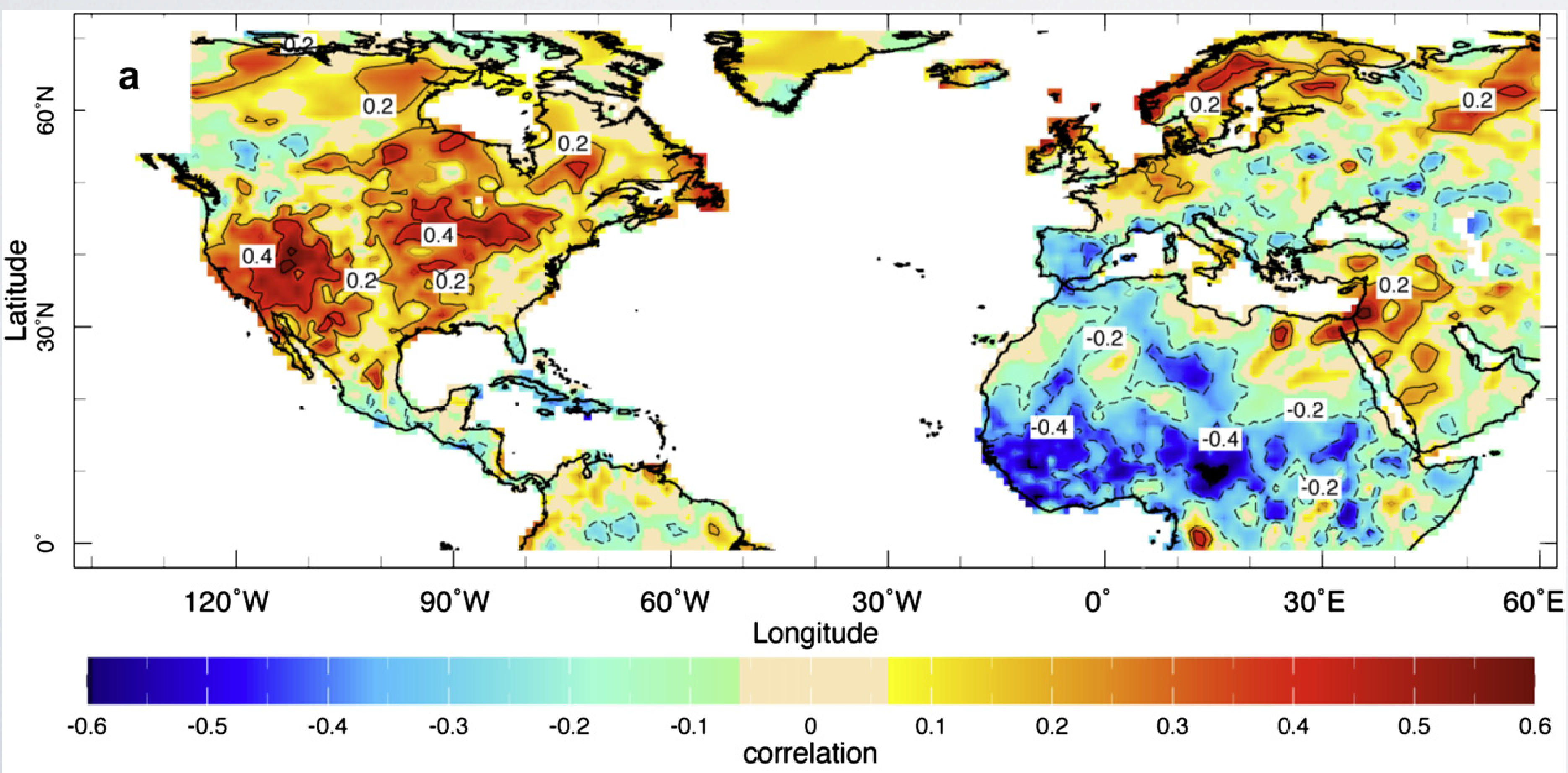

The correlation between annual (October-September) precipitation in Jerusalem and annual precipitation in other Northern Hemisphere land areas. Data are from GPCC with 1° latitude by longitude resolution for the years 1920-1996. All anomalies were calculated with respect to the entire period of analysis and smoothed in time with a 2-nd order binomial filter, which emphasized fluctuations with periods >5-years. A correlation of 0.38 is significant at the 5% level (non-directional) assuming every fourth sample in the record is independent of the others.

Figures: Kushnir and Stein (2010)

THE DEAD SEA: PALEO INDICATOR OF THE LEVANT HYDROCLIMATIC VARIABILITY

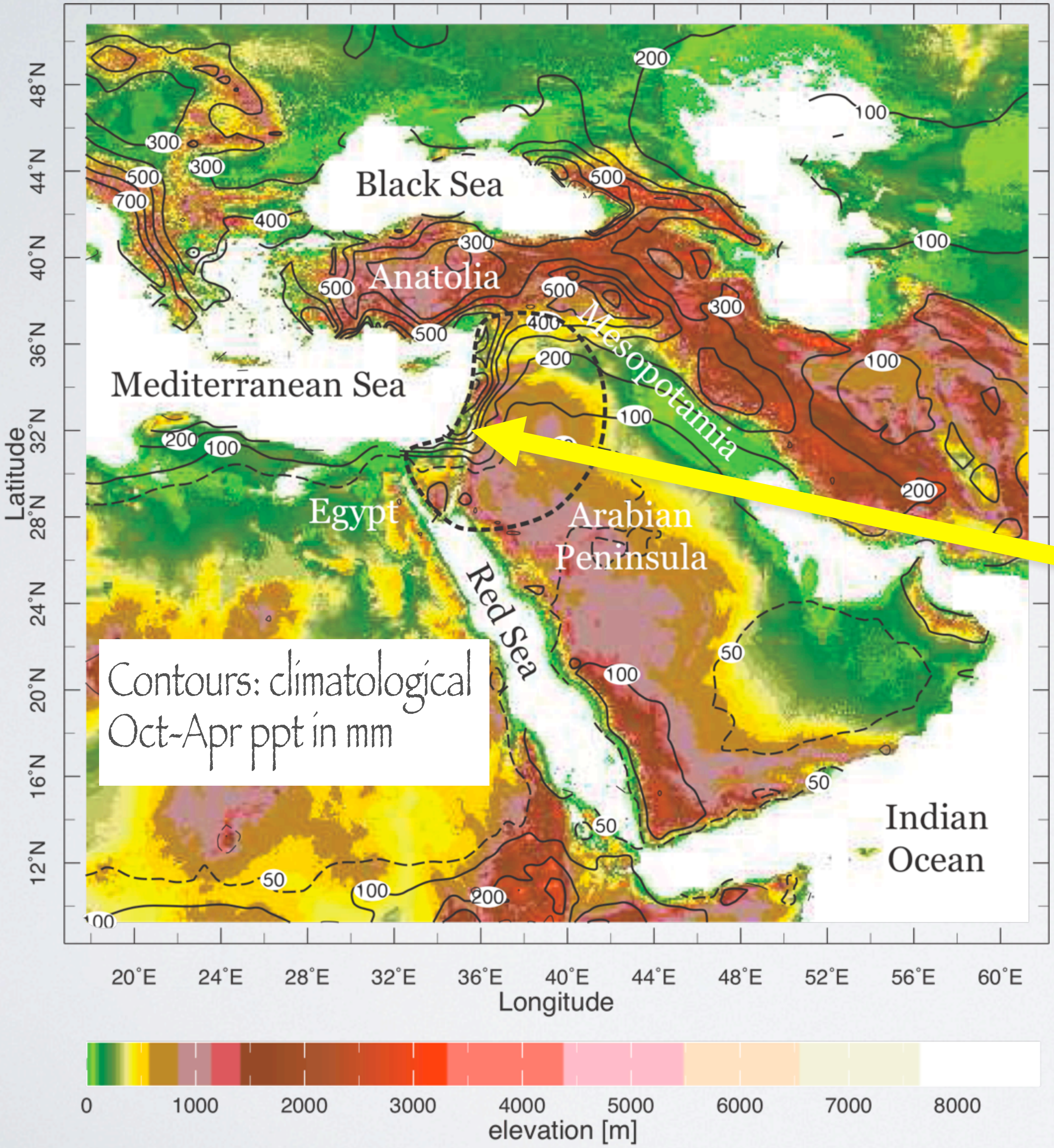

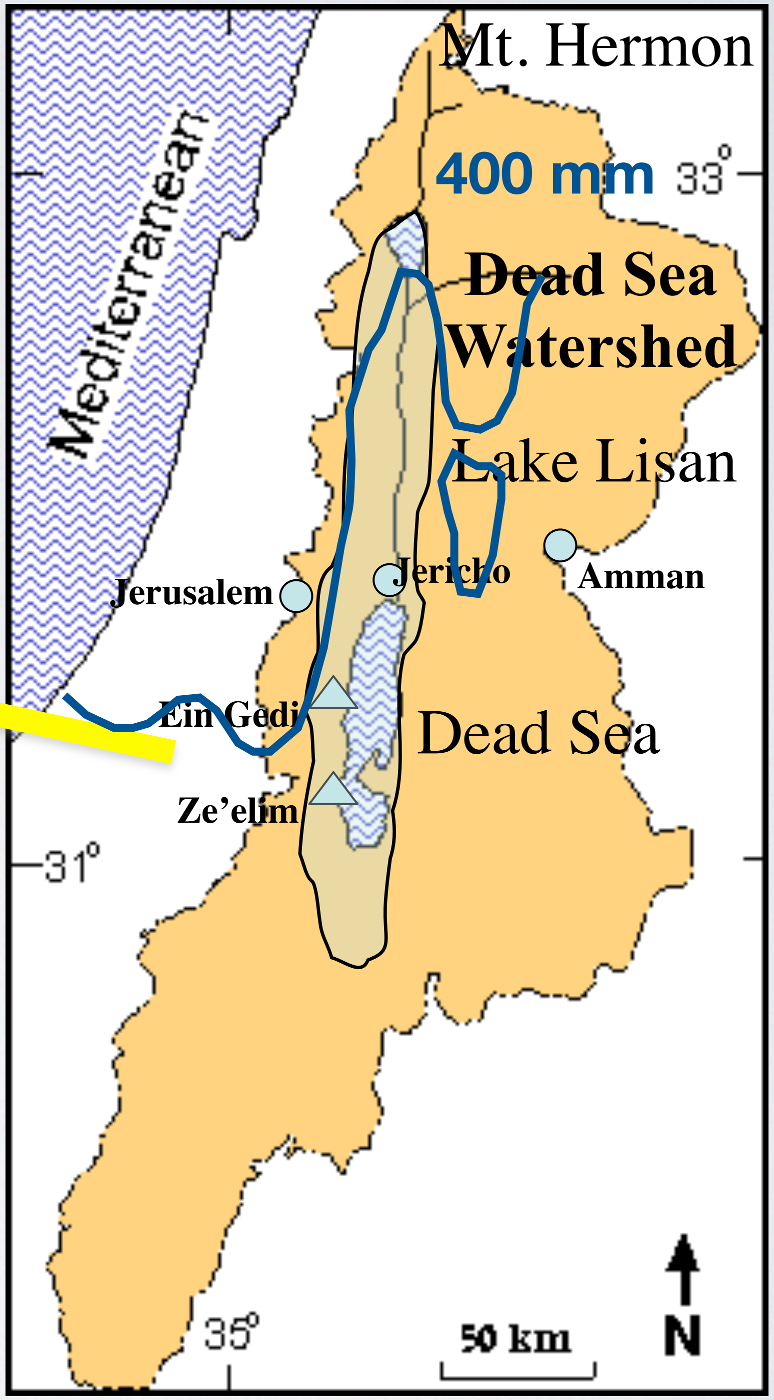

BACKGROUND: LATE HOLOCENE EVIDENCE CONFIRMS LEVANT LINK TO NO. ATLANTIC SSTS

Red shaded strip indicates the timing of the Medieval Climate Anomaly

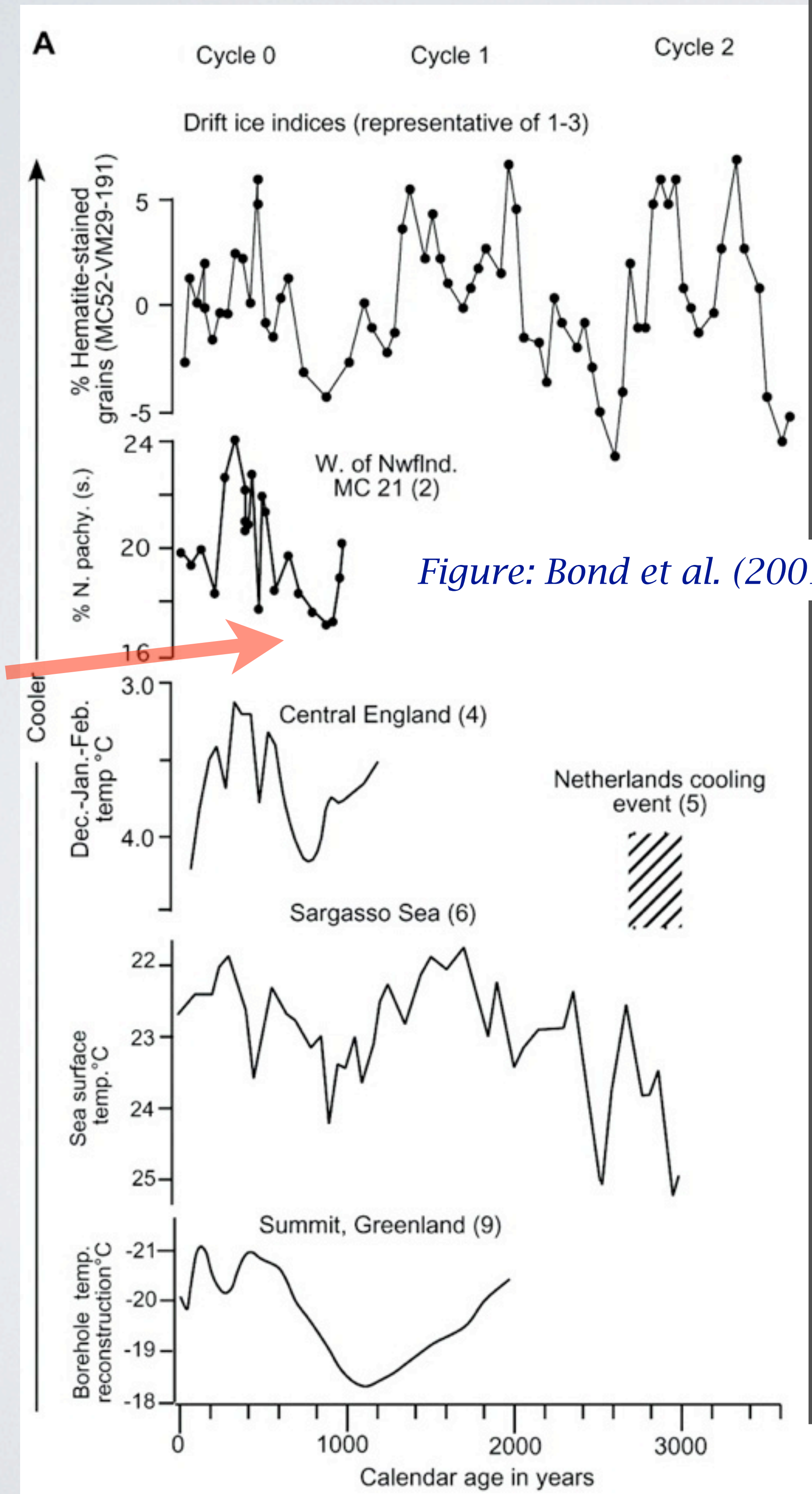

Figure: Bond et al. (2001)

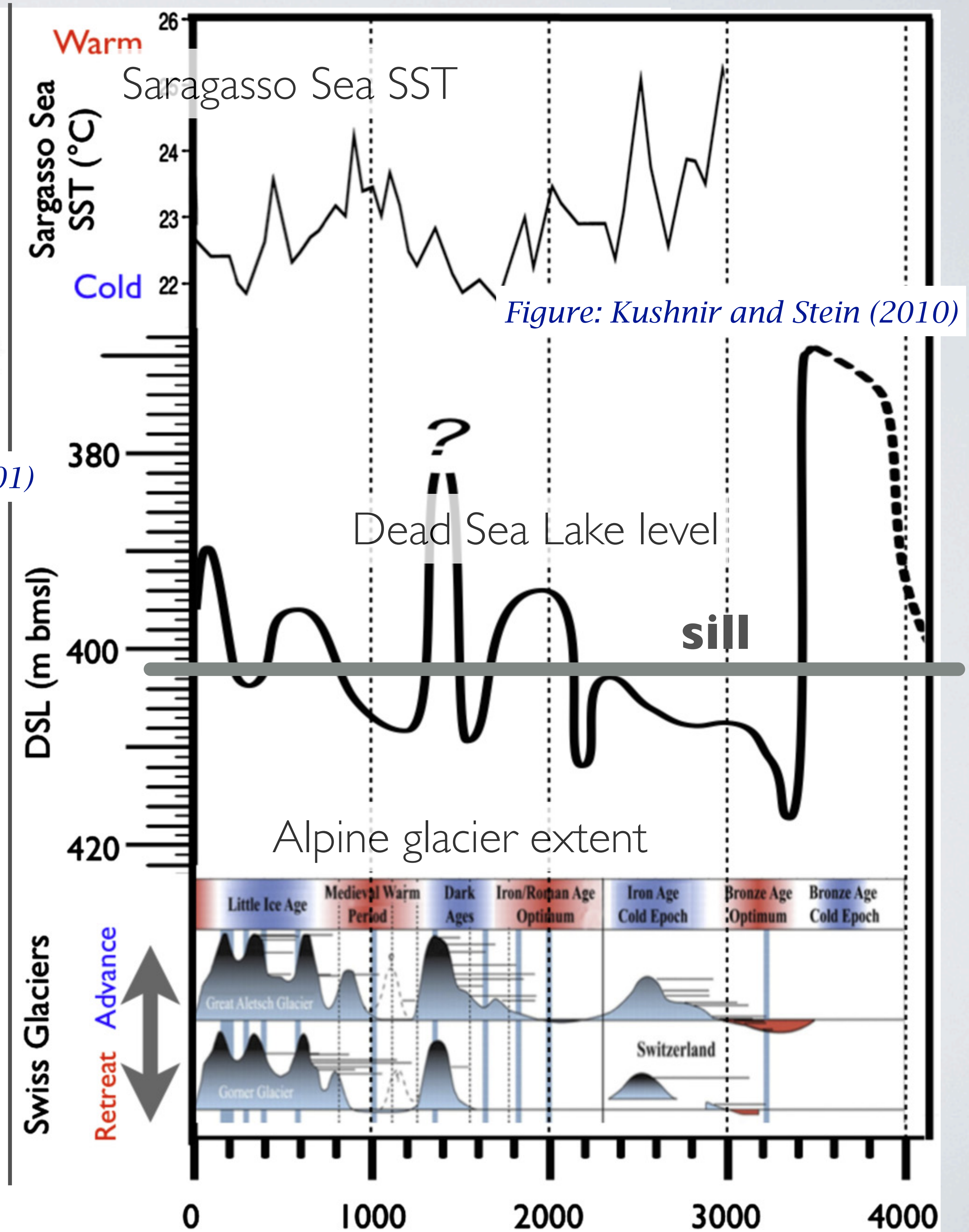

Figure: Kushnir and Stein (2010)

BACKGROUND: LATE HOLOCENE EVIDENCE CONFIRMS LEVANT LINK TO NO. ATLANTIC SSTS

Red shaded strip indicates the timing of the Medieval Climate Anomaly

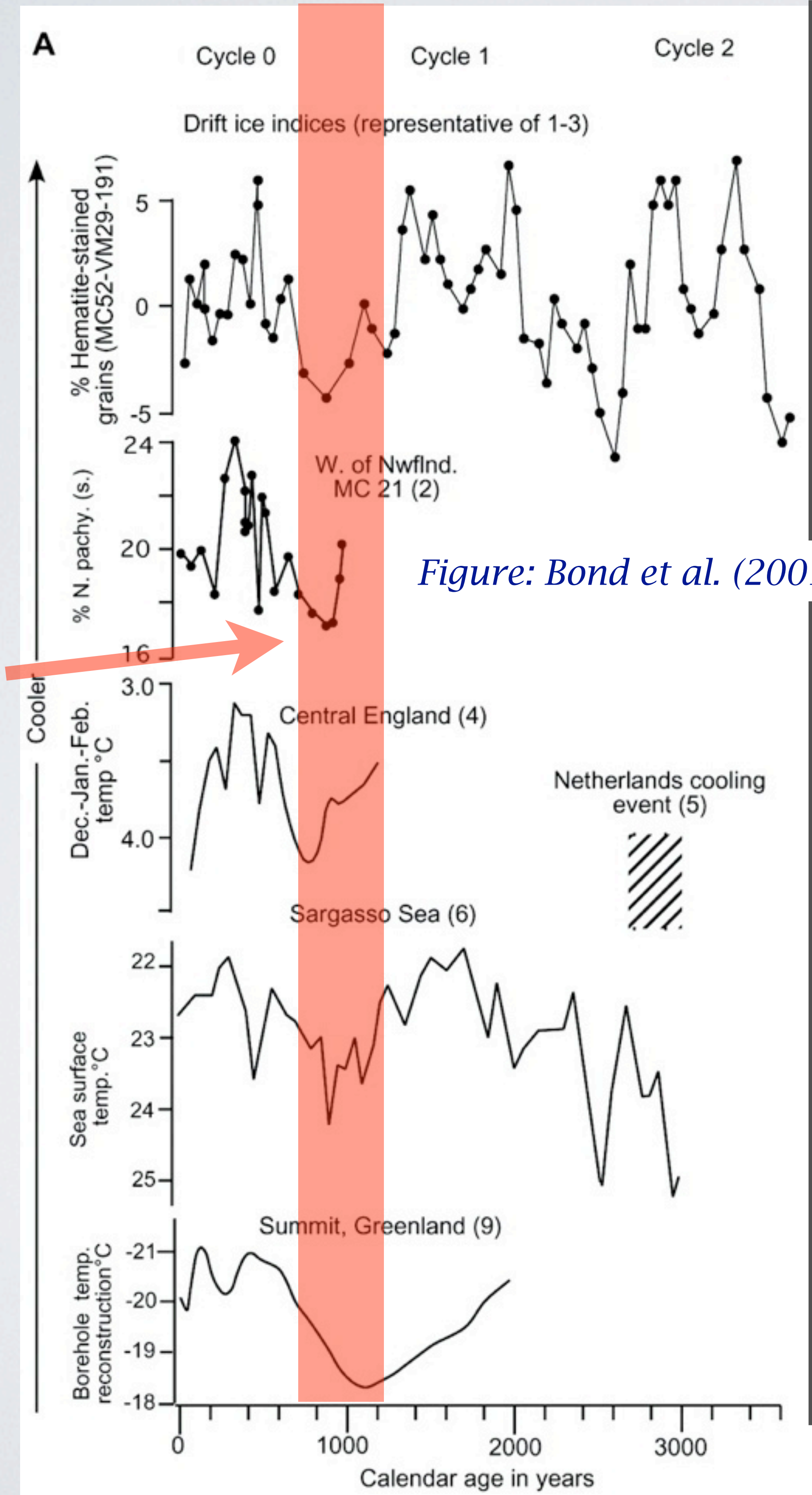

Figure: Bond et al. (2001)

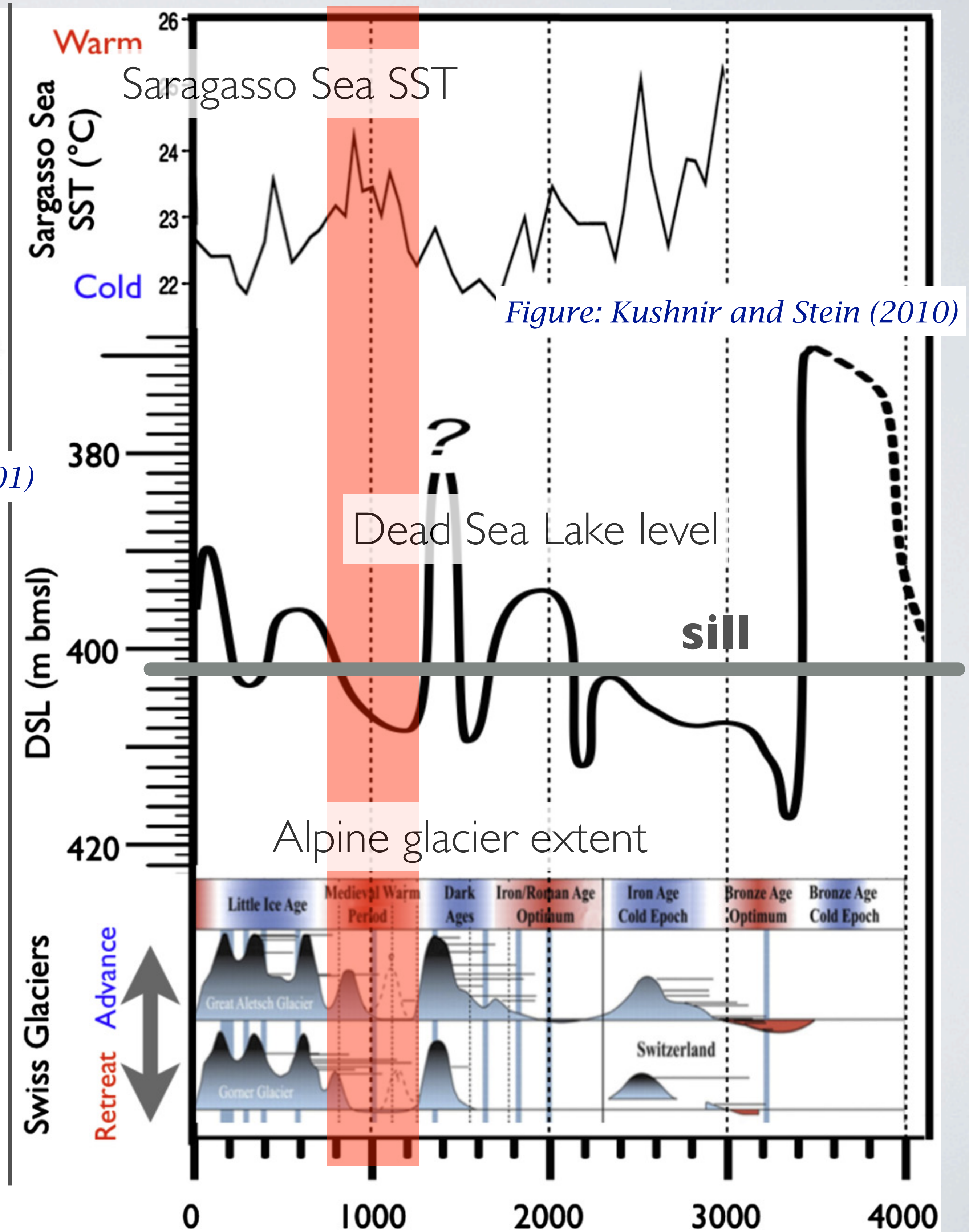

Figure: Kushnir and Stein (2010)

THE NILE

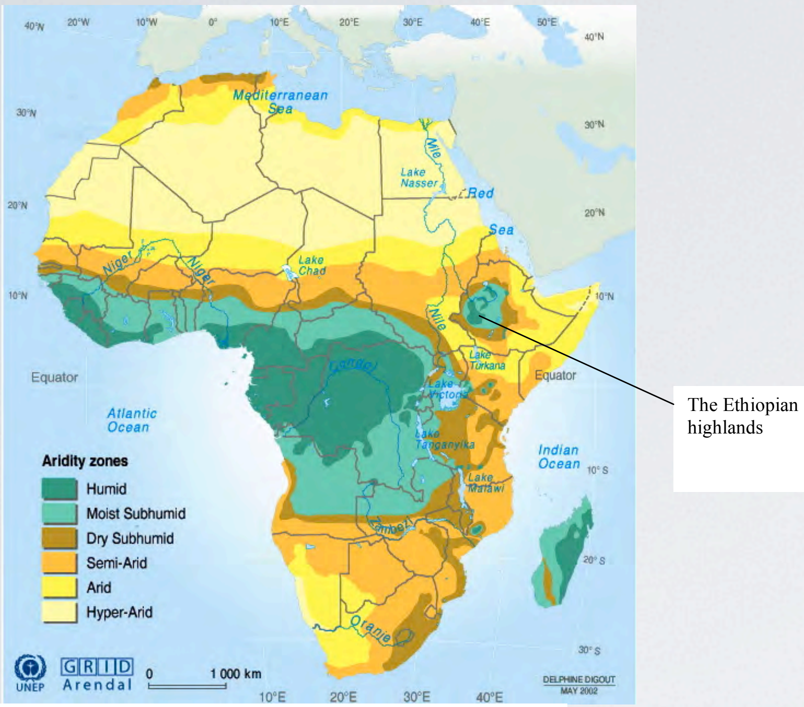

Annual cycle of the Nile flow at Khartoum, where the White and Blue Niles meet. The White Nile flows all year and controls the low-flood levels. The Blue Nile is fed by the summer monsoon rains and determines the high stands between July and November.

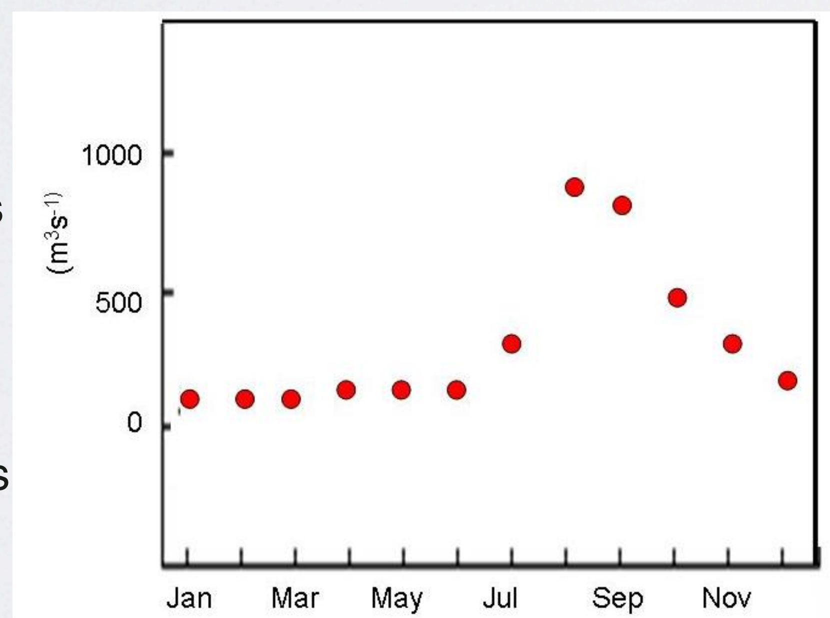

Figure: Feliks (personal comm.)

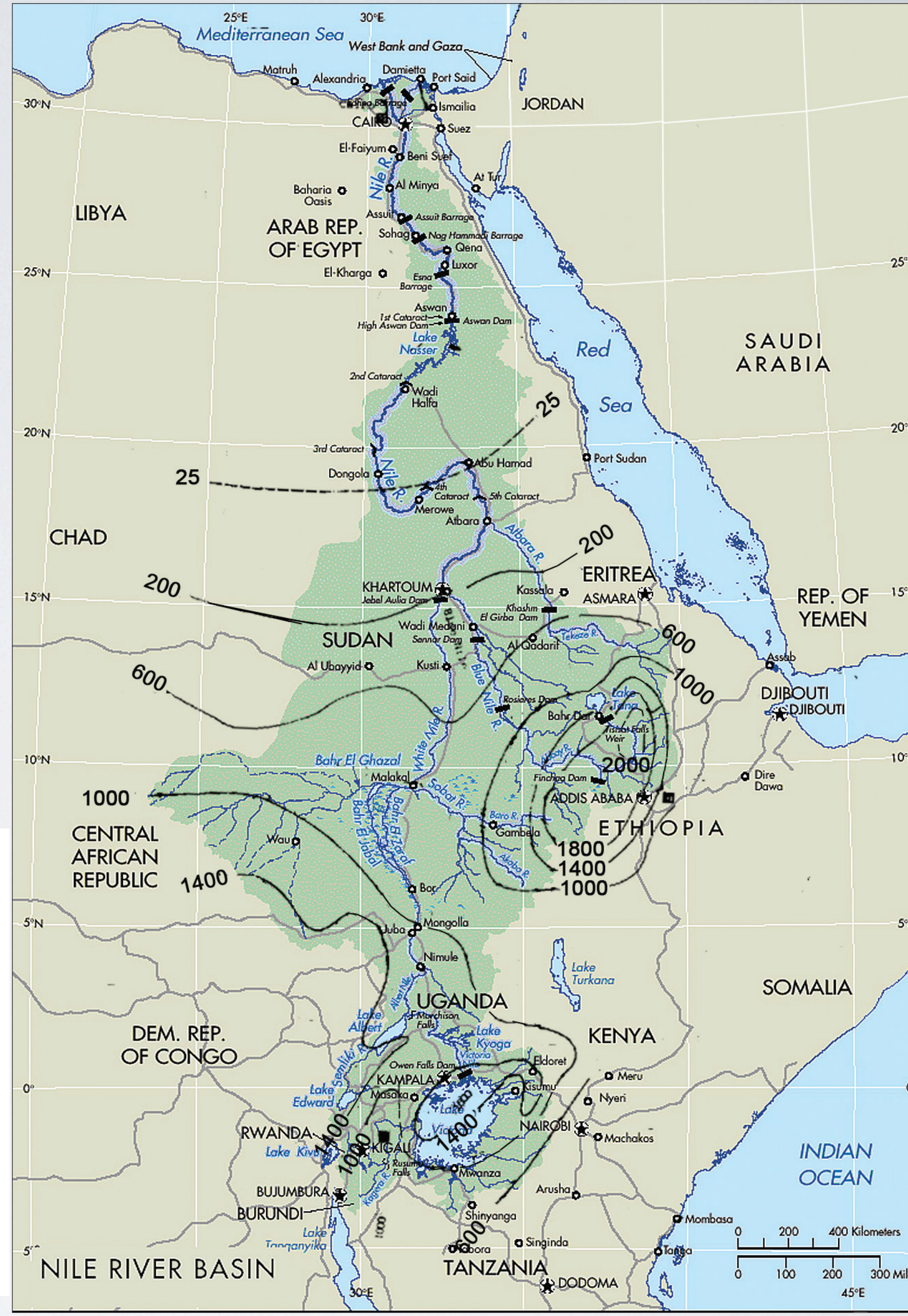

Nile River Basin showing mean annual rainfall in mm in the main Nile catchment areas in Ethiopia and Equatorial Africa. The main tributaries are the White Nile - originating in equatorial E. Africa and the Blue Nile - flowing north from the Ethiopian Highlands.

THE NILOMETER

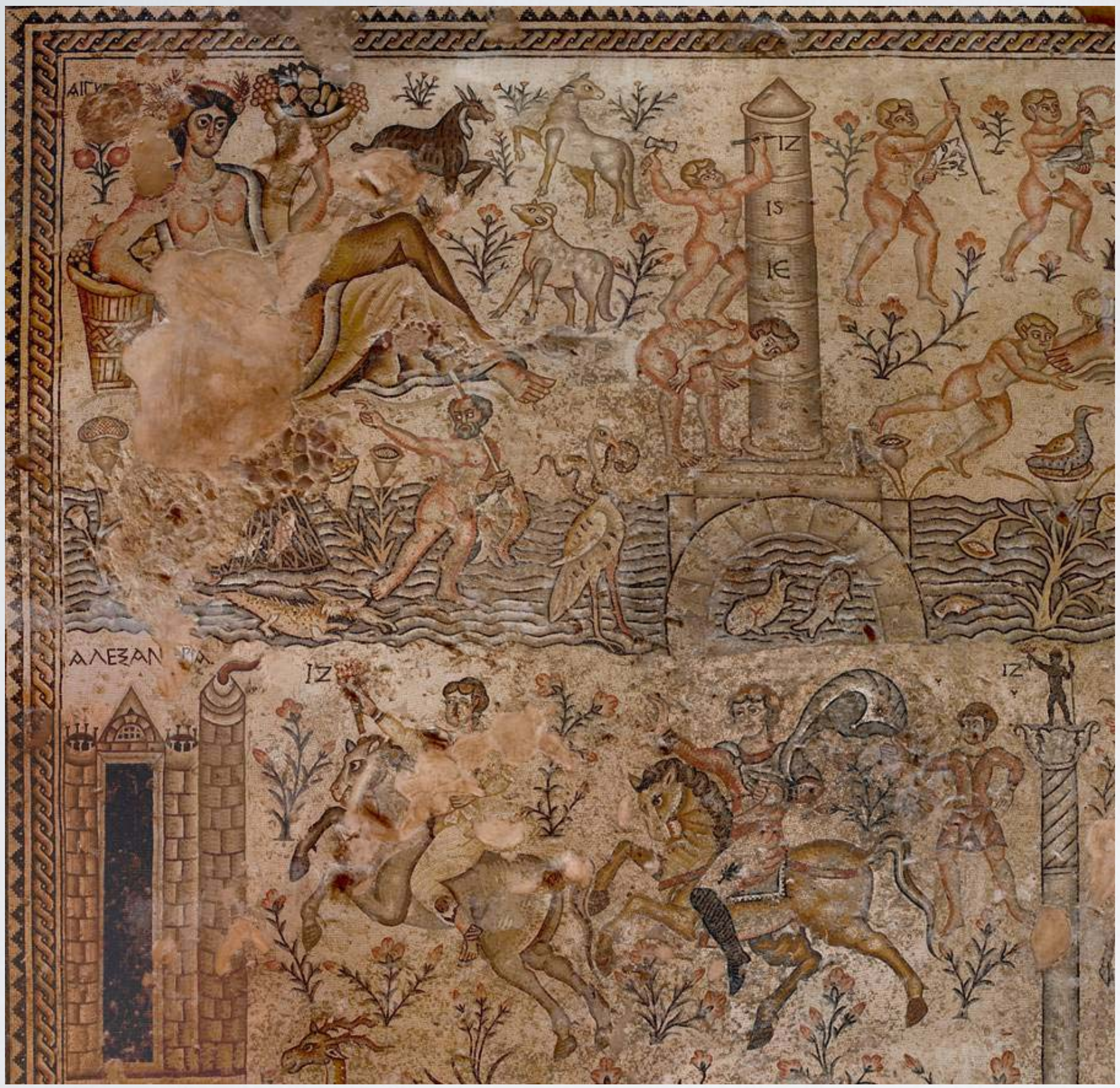

The Nile flood celebration depicted on a 5th century AD mosaic found in Tzipori, Galilee. The Nilometer is at the top and right of center (*photographed by Yigal Feliks, 2005*)

THE NILOMETER ON RAWDA (RODA) ISLAND IN CAIRO (from http://www.touregypt.net/featurestories/nilometerroda.htm)

Nile high and low flood levels monitoring: The most complete records begin at the time the Arabs took control of the country in A.D. 622. They were compled by Toussoun (1925) with additional data by Ghaleb (1951) and Hurst (1952). The data were corrected to account for changes in the unit of length (the cubit), the rise of the bed of the Nile through siltation, and the differences in lunar and solar calendars by Popper (1951).

MEDIEVAL LEVANT DROUGHTS

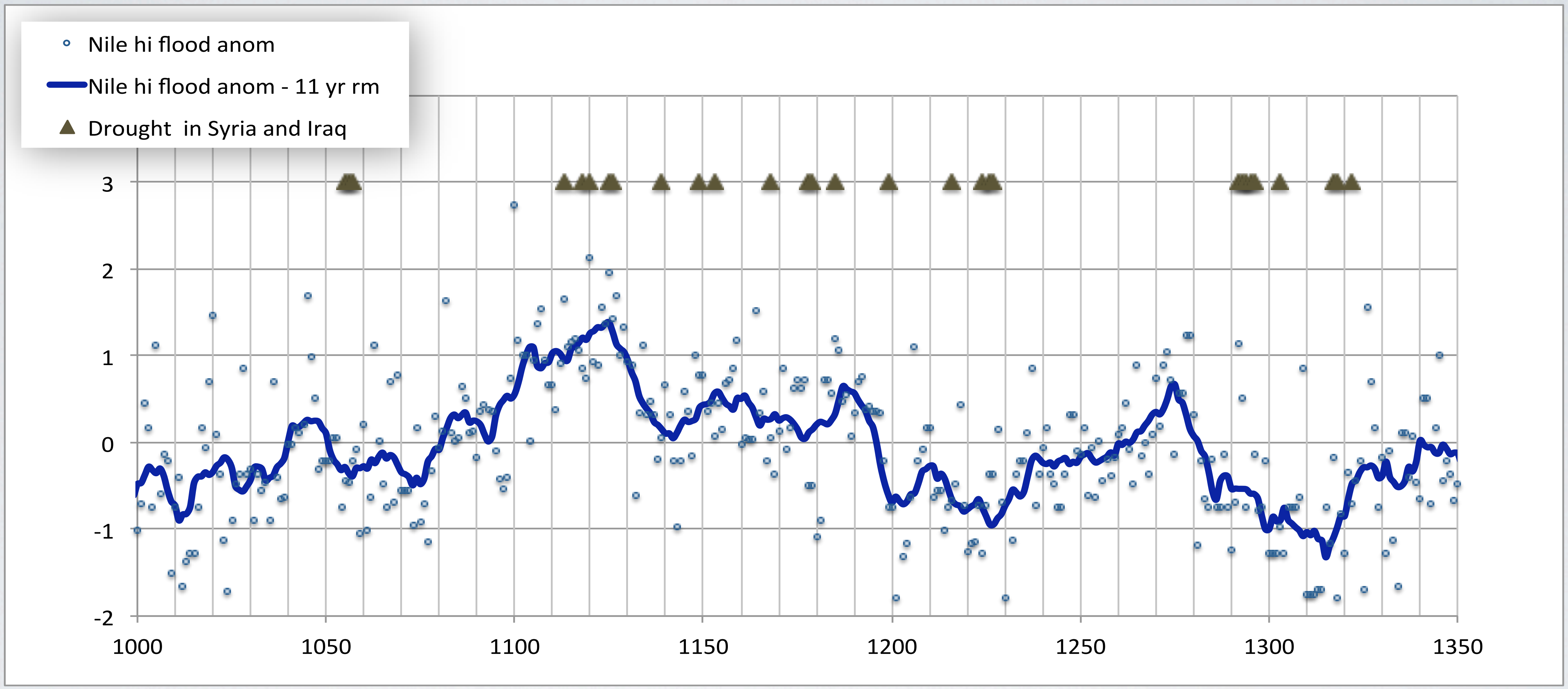

MEDIEVAL LEVANT DROUGHTS

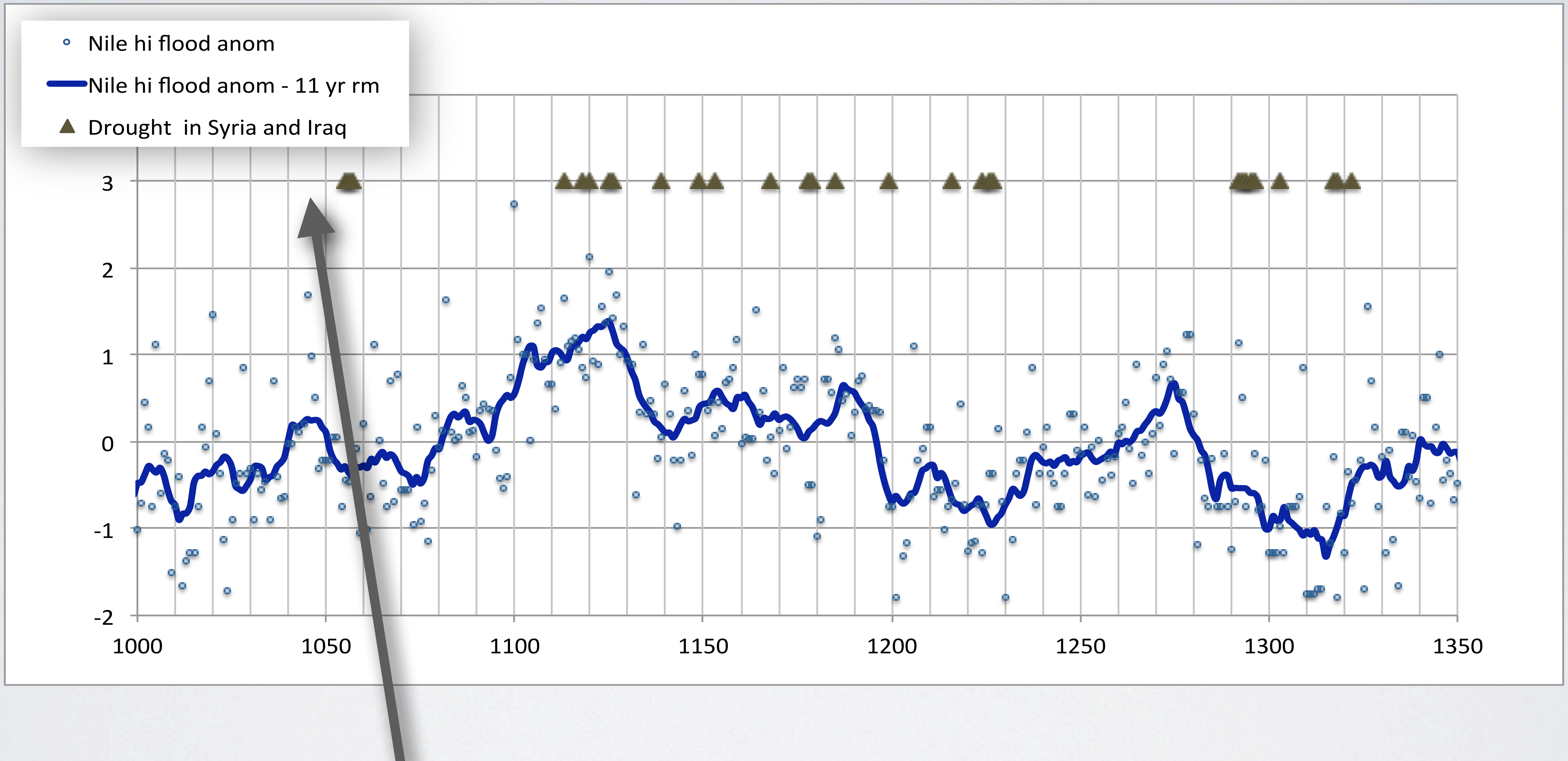

In 1047 Nāṣer-e Khosraw, the Persian poet and theologian, author of the *Safarnāma* ("Book of Travels") describes prosperous villages along the Jerusalem hills, their high yields and low prices. He is convinced that Jerusalem and Syria have never experienced a famine.

MEDIEVAL LEVANT DROUGHTS

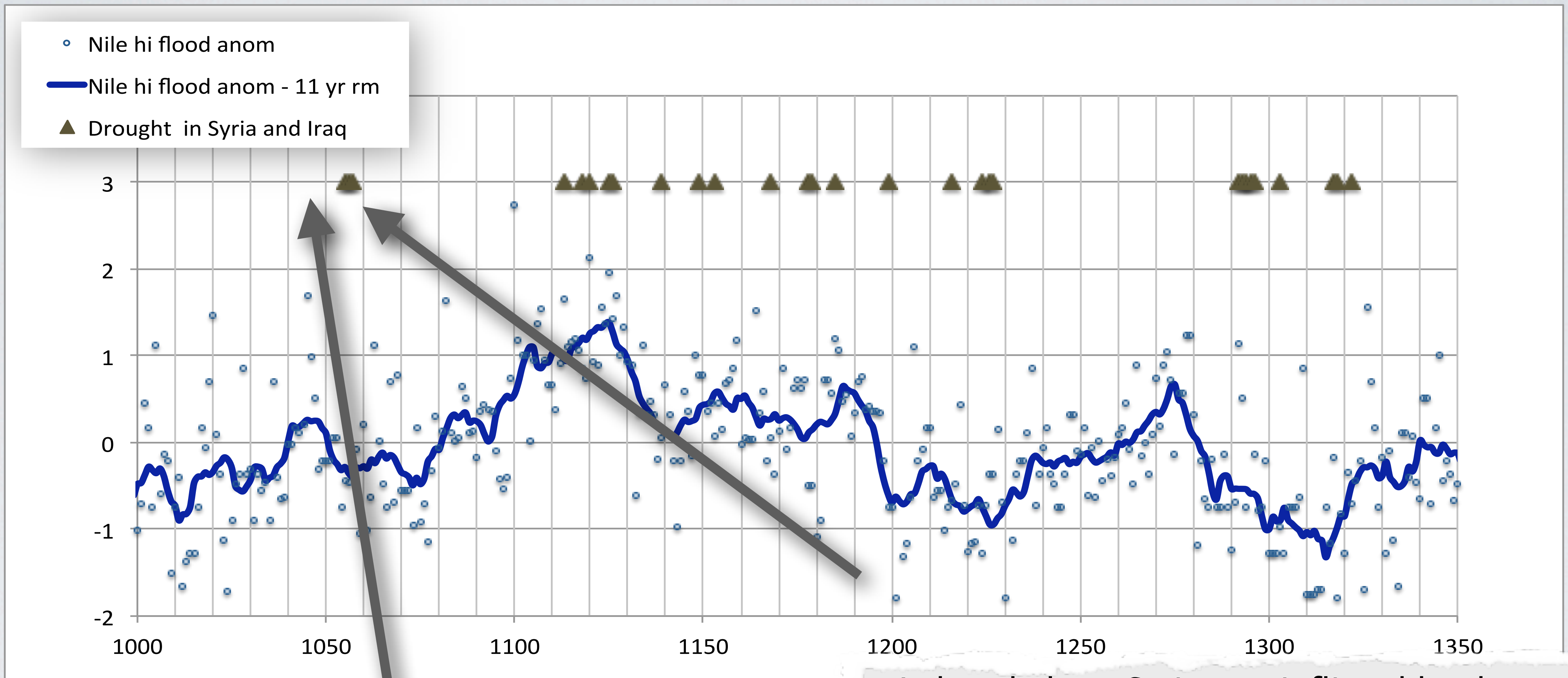

In 1047 Nāṣer-e Khosraw, the Persian poet and theologian, author of the *Safarnāma* ("Book of Travels") describes prosperous villages along the Jerusalem hills, their high yields and low prices. He is convinced that Jerusalem and Syria have never experienced a famine.

A decade later Syria was inflicted by three large-scale droughts (1056, 1077 and 1086). The first was the worst; it stretched over the entire eastern Mediterranean Basin as well as Persia, and the central Asian cities of Bukhara and Samarkand. Plague soon followed, claiming in some regions a third of the population (The Chronography of Bar Hebraeus, tran. E. A. Wallis Budge (Gorgias Press, Piscataway 2003), vol. 1: 209).

A survey of contemporary medieval sources from 1050-1400 reveals a high number of droughts in the Levant during the second half of the 11th century and all through the 12th century. *Thirty-eight droughts* are recorded over this period. *Fifteen of these droughts resulted in famines*. The worst and most frequent famines occurred in the 12th century. Their severity is judged by the size of the territory they covered, the duration and impact on the local population (see Supplement). Several of these droughts stretched over vast regions and lasted over two years leading to destruction of villages, large scale migration, acute famine, sickness and high death tolls.

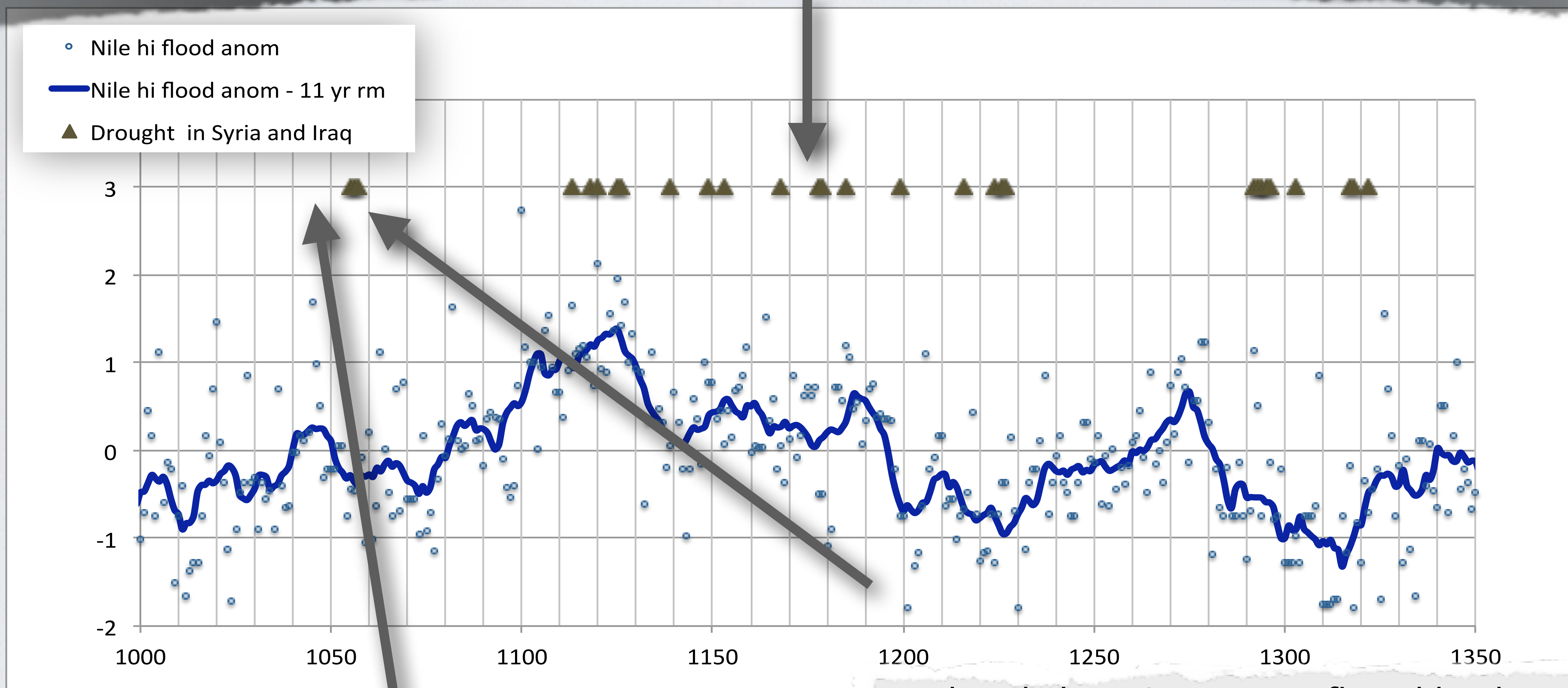

In 1047 Nāṣer-e Khosraw, the Persian poet and theologian, author of the *Safarnāma* ("Book of Travels") describes prosperous villages along the Jerusalem hills, their high yields and low prices. He is convinced that Jerusalem and Syria have never experienced a famine.

A decade later Syria was inflicted by three large-scale droughts (1056, 1077 and 1086). The first was the worst; it stretched over the entire eastern Mediterranean Basin as well as Persia, and the central Asian cities of Bukhara and Samarkand. Plague soon followed, claiming in some regions a third of the population (The Chronography of Bar Hebraeus, tran. E. A. Wallis Budge (Gorgias Press, Piscataway 2003), vol. 1: 209).

One of the most striking accounts that reveal the climatic change and the arrival of the "Medieval Climate Anomaly" in the Middle East was written by William Archbishop of Tyre (c.1130-1185), the court historian of the first Crusader Kingdom:

"The city (Jerusalem) lies in arid surroundings, entirely lacking in water. Since there are no rills, springs or rivers, the people depend upon rain water only. During the winter season it is their custom to collect this in cisterns, which are numerous throughout the city. Thus it is preserved for use during the year. Hence, I am surprised at the statement of Solinus (c. mid 4th century A.D.) that Judea is famous for its waters. He says in the Polyhistor "Judea is renowned for its waters, but the nature of these varies." I cannot account for this discrepancy except saying either that he did not tell the truth about the matter or that the face of the earth became changed later." (William of Tyre, Beyond the Sea, vol. 1, Book 8: 346-347.)

DSL + LEVANT & NILE VALLEY DROUGHTS

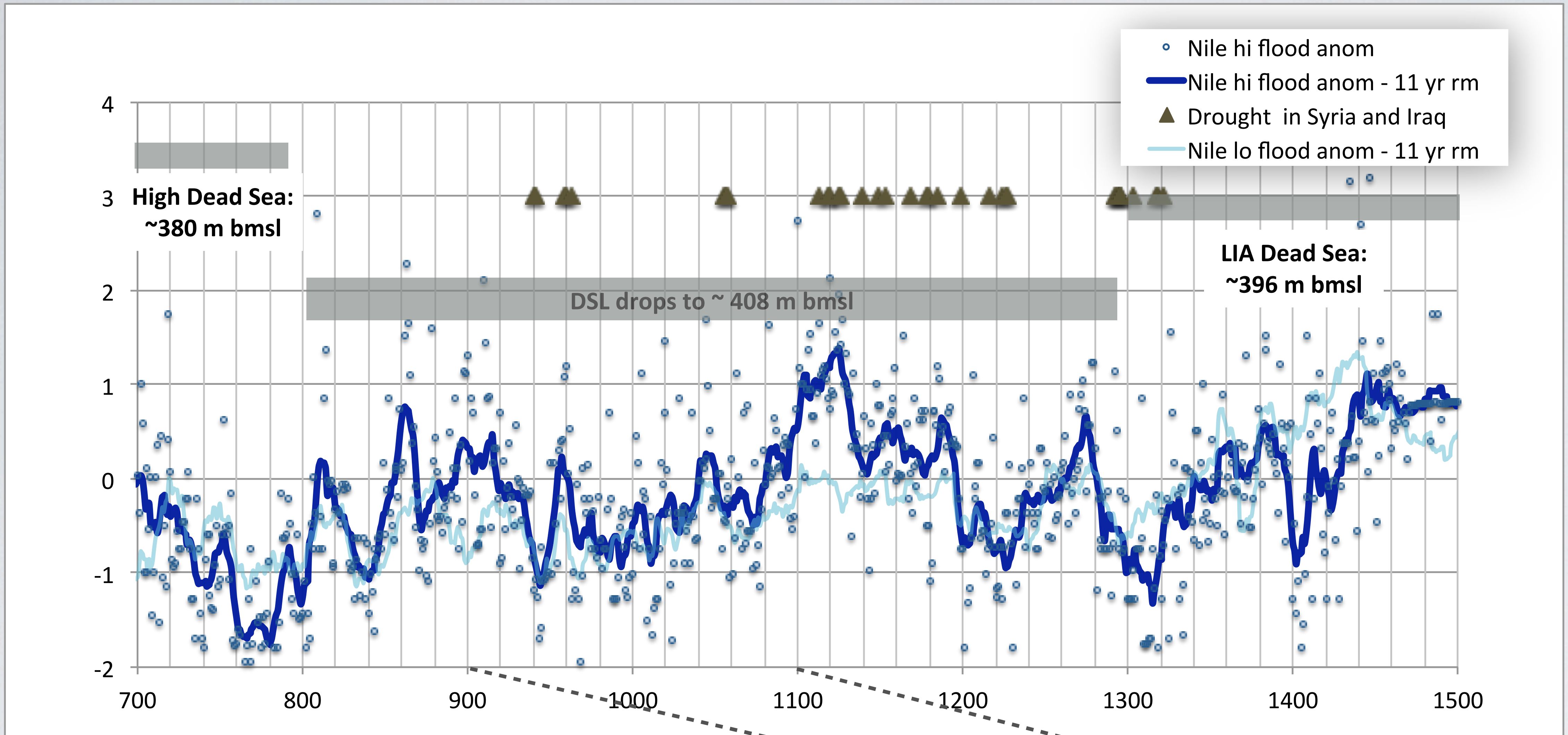

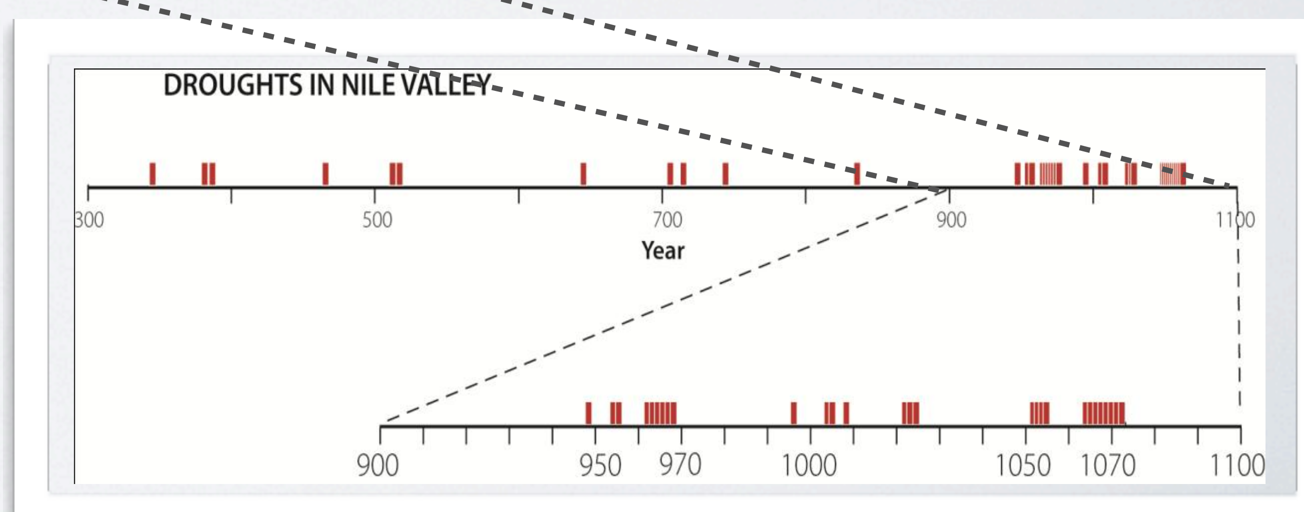

The record of severe droughts in the Nile Valley 400-1100 AD, as determined from historical documents. Source: "The collapse of the eastern Mediterranean" by R. Ellenblum, The Hebrew University of Jerusalem (Cambridge University Press to appear in spring 2012).

SUMMARY

- Historical documents help pin down accurately the timing of significant climatic events.
- They add a human description to indirect evidence imprinted in the natural environment, i.e., the biological, geological, and geochemical proxies.
- In this case they confirm the impression, based on the the DSL record, of a marked drawdown of precipitation in the Middle East / Levant region during the MCA.
- Through comparing documentary evidence with physical observations (i.e., recorded annual flood levels of the Nile) we also confirm the multidecadal time scale, negative correlation, between Levant rainfall and the strength of the African summer monsoon.